ADVANCES IN INORGANIC CHEMISTRY, VOL. 45

# STRUCTURE–FUNCTION CORRELATIONS IN HIGH-POTENTIAL IRON PROTEINS

J. A. COWAN and SIU MAN LUI

Evans Laboratory of Chemistry, The Ohio State University, Columbus, Ohio 43210



## I. Scope of the Review

High-potential iron proteins (HiPIPs) comprise a subset of the 4Fe–4S cluster family of metalloproteins that are characterized by a positive reduction potential, $E_m$, in the range of +50 to +450 mV. This class is differentiated from the 4Fe–4S centers in low-potential ferredoxins, which show a negative $E_m$, typically varying between −100 and −650 mV. The origin of these distinct redox properties has been rationalized in terms of the three-state hypothesis of Carter (*1*), summarized in Scheme 1, and can be attributed to the stability of the common $[Fe_4S_4(SR)_4]^{2-}$ state.

The physical biochemistry of these two classes of 4Fe–4S proteins has been extensively studied and reviewed, especially with regard to redox and electron transfer chemistry (*2–22*), whereas the magnetic properties of the cluster have been probed by electron paramagnetic resonance (EPR) (*23–34*), nuclear magnetic resonance (NMR) (*24*, *25*, *35–54*), and susceptibility measurements (*56–61*). Mössbauer spec-




0898-8838/98 $25.00

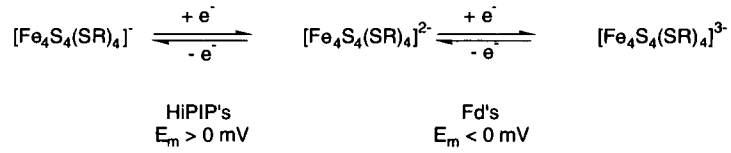


**Scheme 1**

troscopy has also been used extensively to investigate the distribution of valence states over the four iron centers (*24*, *27*, *32*, *33*, *62–68*).

This review will not dwell on the aforementioned "classical" areas of investigation, nor on more recent theoretical developments in magnetic coupling schemes that advance understanding of the electronic and magnetic properties of such centers. These topics have received extensive coverage elsewhere (*45*, *56*, *58*, *69–74*), including a series of concise commentaries in Ref. *55*, and interested readers are directed to this literature. Rather, this article will focus on more recent developments in understanding structure–function relationships for these proteins; including natural *in vivo* function, recent structural advances through X-ray and NMR solution studies, and new insights on the functional roles of amino acid residues in the control of cluster stability and redox chemistry. Although model complexes will not be a focus of this review, per se, reference will be made to results obtained from such investigations when they complement, and lend additional insight into, data from protein studies. The literature on synthetic cluster chemistry has also been the subject of review (*75–78*).

## II. Source and Function of HiPIPs

The 4Fe–4S cluster proteins have now been identified in a large number of functional contexts, varying from a structural or sensory role in RNA- and DNA-binding and repair proteins or enzymes (*79–84*), and metabolic enzymes (*85*), including catalysis of hydrolyase isomerization reactions (*86*, *87*). In the facultative anaerobe *Escherichia coli* the transcription factor FNR (fumarate nitrate reduction) regulates gene expression in response to oxygen deprivation (*88–90*). The loss of the Fe–S cluster by exposure to oxygen is accompanied by conversion to the monomeric form of the protein and decreased DNA binding, suggesting that oxygen regulates the activity of wild-type FNR through the lability of the Fe–S cluster to oxygen (*90*). A plausible mechanism for such lability is discussed in Section IV,A,1. Clearly, these functional activities are distinct from traditional elec-

tron transfer reactions (*6*, *7*, *9*, *11*, *19*, *21*, *43*, *48*, *51*, *71*, *73*, *91–97*). Table I provides a summary listing of proteins with no electron transfer role, and their functional characteristics. For those proteins where a structural role in a DNA-binding protein is suggested, the cluster appears to be nonredox active, and so it is difficult to define the cluster as a high- or low-potential center. In other cases, oxidation of the cluster is accompanied by loss of a labile Fe to generate a 3Fe–4S center (*28*, *83*, *84*, *98–101*). The factors underlying the stability of oxidized $[Fe_4S_4(SR)_4]^-$ clusters will be discussed later.

Table II summarizes the sources and key properties of isolated HiPIPs, almost all of which have been isolated from photosynthetic organisms, and there has been extensive speculation on their involvement in respiratory electron transport chains (*18*, *21*, *91–93*, *95*, *96*, *102–105*). Evidence in support of such a hypothesis has recently emerged from studies of a partially reconstructed reaction center (RC) complex from *Rhodoferax fermentans* (*93*, *95*). The kinetics of photoinduced electron transfer from HiPIP to the reaction center suggested the formation of a HiPIP–RC complex with a dissociation constant of 2.5 $\mu M$. *In vivo* and *in vitro* studies by Schoepp *et al.* (*94*) similarly have demonstrated that the only high-redox-potential electron transfer component in the soluble fraction of *Rhodocyclus gelatinosus* TG-9 that could serve as the immediate electron transfer donor to the reaction-center-bound cytochrome was a HiPIP. *In vitro* experiments have shown HiPIP to be an electron donor to the *Chromatium* reaction center (*106*). Fukumori and Yamanaka (*107*) also reported that *Chromatium vinosum* HiPIP is an efficient electron acceptor for a thiosulfate-oxidizing enzyme isolated from that organism.

TABLE I

CLASSES OF 4FE–4S-CONTAINING PROTEINS WITH NONREDOX ROLES[a]

| Protein | Protein function | Cluster function |
|---|---|---|
| Aconitase (*28*, *100*) | Isomerase | Catalytic |
| Lysine 2,3-amino mutase (*86*) | Enzyme | Catalytic |
| Glutamine phosphoribosyl pyrophosphate amidotransferase (*85*) | Enzyme | Structural |
| Endonuclease III (*81*) | DNA repair | Structural |
| Transcription factor FNR (fumarate nitrate reduction) (*90*) | Transcriptional regulation | Sensory |
| Iron-response protein (IRP) (*83*, *84*) | Translational regulation | Sensory |
| Mut Y (*79*) | DNA repair | Structural |

[a] Some data is from Ref. *80*.

TABLE II

SOURCES AND KEY PROPERTIES OF HiPIPs[a]

| Source | $E_m$ (mV) | No. of residues | Net charge[b] |
|---|---|---|---|
| **Chromatiaceae** | | | |
| *Chromatium purpuratum* (*91*) | +390 | —[c] (dimeric?) | —[c] |
| *Chromatium tepidum* (*123*) | +323 | 83 | −4 |
| *Thiocapsa roseopersicina* (*103, 105, 173, 174*) | +346 or +325 | 85 | −6 |
| *Chromatium warmingii* (*175*) | +355 | 85 | −4 |
| *Chromatium vinosum* (*138*) | +356 | 85 | −5 |
| *Chromatium gracile* (*39, 173*) | +350 | 83 | −7 |
| Thiocapsa pfennigii (176) | +352 | 81 | −9 |
| **Ectothiorhodospiraceae** | | | |
| *Ectothiorhodospira halophila* (*11, 161, 177*) | +120 (iso I) | 71 | −12 |
| *Ectothiorhodospira vacuolata* (*161, 172*) | +260 (iso I) | 72 | −5 |
| | + 150 (iso II) | 71 | −8 |
| *Ectothiorhodospira shaposhnikovii* (*172*) | +270 (iso I) | 72 | −6 |
| | +155 (iso II) | 71 | −8 |
| **Rhodospirillaceae** | | | |
| *Rhodoferax fermentans* (*21, 93, 95*) | +351 | —[c] | —[c] |
| *Rhodopila globiformis* (*159, 161*) | +450 | 57 | −3 |
| *Rhodospirillum salinarum* (*17, 172*) | +265 (iso I) | 57 | −5 |
| | —[c] (iso II) | 54 (hexameric) | −1 |
| *Rhodopseudomonas marina* (*96*) | +345 | 53 | +5 |
| *Rhodocyclus tenuis* (*114, 159, 172*) | +300 | 62 | +2 |
| *Rhodomicrobium vannielii* (*172*) | —[c] | 53 | +4 |
| *Rhodocyclus gelatinosus* (*35, 94, 161*) | +332 | 74 | +3 |
| **Denitrifying bacteria** | | | |
| *Paracoccus halodenitricans* (*178*) | +282 | 71 | −13 |
| **Aerobic sulfur bacteria** | | | |
| *Thiobacillus ferrooxidans* (*26, 159, 179, 180*) | +380 | 53 (tetramer) | +1 |

[a] Data from Ref. *172*.

[b] Net charge of the peptide chain assuming His to be protonated and the Cys to be ionized. The charge on the cluster is omitted.

[c] Not determined.

## III. X-Ray and Solution Structures

### A. AVAILABLE STRUCTURAL DATA

Most high-potential iron proteins have been isolated from purple photosynthetic bacteria and vary in size from 6 to 10 kDa; the tertiary structures of many have been determined in the crystalline and/or solution states, including HiPIPs from *C. vinosum* (*1, 49, 52, 108–110*), *Ectothiorhodospira halophila* I (*48, 102, 111, 112*), *Ectothiorhodospira*

*vacuolata* II (*113*), and *Rhodocyclus tenuis* (*114*). The availability of high-resolution structural data allows identification of common structural traits that may be of functional significance for cluster chemistry, and that may also be subsequently investigated by site-directed mutagenesis. Such experiments have allowed the various contributing factors to cluster chemistry to be disentangled and their relative importance gauged (Section IV). A similar use of recombinant DNA techniques has also been made in studies of the coordination environment of iron–sulfur centers in low-potential ferredoxins (*115*).

Table III summarizes the sources of available X-ray and solution structural data on HiPIPs. In general there appears to be no significant variation between the solid state and solution structures. Bertini and co-workers have provided the solution structures of both reduced and oxidized HiPIPs (*48*, *112*, *116*), advancing the standard NMR methodologies to paramagnetic proteins (*53*). In agreement with the X-ray studies, they found structural similarities between the two states at different oxidation levels (*117–119*), consistent with the general design concept of electron transfer proteins.

## B. Structure–Function Correlations

### *1. Primary Structure*

The structures of the 4Fe–4S clusters in HiPIPs and low-potential ferredoxins (Fds) are very similar; however, there are major differ-

TABLE III

High-Resolution Structures of HiPIPs

| Source of HiPIP | X-Ray or NMR | Resolution (Å) |
|---|---|---|
| *Chromatium vinosum* (C77S mutant) (*108*) | $NMR_{red}$ | RMSD, 0.62 ± 0.9 (backbone)<br>1.09 ± 0.11 (heavy atoms) |
| *Ectothiorhodospira halophila* I (*48*) | $NMR_{ox}$ | RMSD, 0.67 ± 0.46 (backbone)<br>1.23 ± 1.06 (heavy atoms) |
| *Chromatium vinosum* (*49*) | $NMR_{ox}$ | RMSD, 0.57 ± 0.14 (backbone)<br>1.08 ± 0.16 (heavy atoms) |
| Chromatium vinosum (*52*) | $NMR_{red}$ | RMSD, 0.62 ± 0.12 (backbone)<br>1.19 ± 0.18 (heavy atoms) |
| *Ectothiorhodospira vacuolata* II (*113*) | $X\text{-}Ray_{ox}$ | 1.8 (*R* factor, 16.3%) |
| *Rhodocyclus tenuis* (*114*) | $X\text{-}Ray_{red}$ | 1.5 (*R* factor, 17.3%) |
| *Ectothiorhodospira halophila* I (*102*) | $X\text{-}Ray_{red}$ | 2.5 (*R* factor, 18.4%) |
| *Chromatium vinosum* (*109*) | $X\text{-}Ray_{ox}$ | 2.0 (*R* factor, 24%) |
| *Chromatium vinosum* (*1, 110*) | $X\text{-}Ray_{red}$ | 2.5 (*R* factor, 24.7%) |

ences in the local environment of the clusters in these two types of proteins. The sequences and folding patterns, the locations of the cysteine residues, and the positions of the hydrogen bonds are very different (*120–122*). For example, the amino acid sequence motif $-CX_2CX_2C \cdot \cdot \cdot X_n \cdot \cdot \cdot C-$ for Fds differs from that of HiPIPs, typically $-CX_2CX_{16}CX_{13}C-$, which in turn differs from the sequence motif for novel cluster-containing proteins such as endonuclease III, with the compact sequence $-CX_6CX_2CX_5C-$. Reviews of protein folding patterns around clusters, and issues related to the evolution of such proteins, have appeared in the literature (*120*, *122*).

*2. Secondary and Tertiary Structure*

Carter has reviewed the comparative crystallography of oxidized and reduced *C. vinosum* HiPIP (*1*), and the dimensional changes of the iron–sulfur cube following oxidation or reduction have also been extensively tabulated and discussed for both model complexes and protein-bound clusters (*118*). In spite of the low sequence homology in HiPIPs, there is a remarkable similarity in tertiary structure, especially around the cluster (*114*). No significant secondary structure is observed in the HiPIPs, with only two short $\alpha$-helical segments, three strands of antiparallel $\beta$-pleated sheet, and one small helix near the N terminus (Fig. 1). The 4Fe–4S cluster is buried in the protein interior and is inaccessible to solvent (Fig. 2). This feature has been pro-

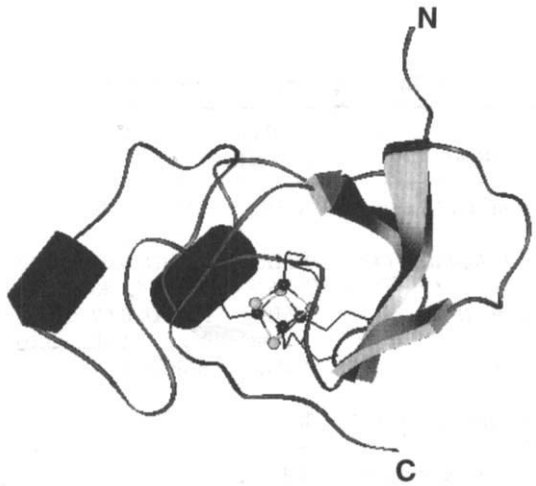


FIG. 1. Secondary and tertiary structural elements of *Chromatium vinosum* HiPIP.

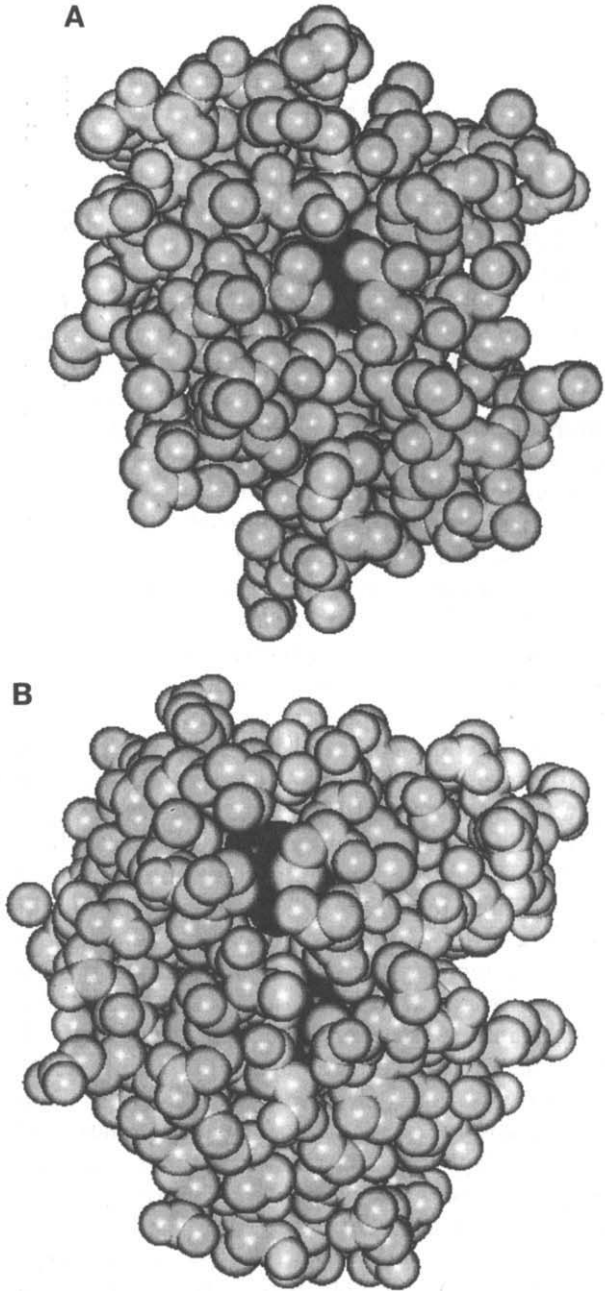


FIG. 2. Exposure of the 4Fe–4S cluster illustrated for high- and low-potential ferredoxins. (A) *Chromatium vinosum* HiPIP; (B) *Azotobacter vinelandii* Fd (the 4Fe–4S cluster is more exposed than the 3Fe–4S center).

posed to account for the stability of the $[Fe_4S_4(SR)_4]^{-/2-}$ oxidation states and the positive reduction potential, relative to the low-potential ferredoxins (*119*). Note, however, from the images in Fig. 2, that it is predominantly the depth of penetration required of solvent, rather than the "exposed" area of the cluster, that is the critical distinction between these protein classes. Finally, the coordinated sulfur atoms in *C. vinosum* HiPIP are involved in five (conserved) H-bond interactions with peptide NH protons, which are maintained in both oxidation states.

Benning *et al.* (*113*) have reported the molecular structure of the oxidized HiPIP (isoform II) from *E. vacuolata*, which shows close similarity to that of other HiPIPs, that is, a series of reverse turns wrapping around an iron–sulfur cluster to form a hydrophobic pocket. These researchers also pointed out that the structure of *E. vacuolata* II HiPIP [net charge = −8 (reduced); $E_m$, +150 mV] is intermediate between *C. vinosum* [net charge = −4 (reduced); $E_m$, + 352 mV) and *E. halophila* I [net charge = −11 (reduced); $E_m$, +120 mV) HiPIPs, based on the pattern of insertions and deletions, overall structural identity, and the percentage amino acid sequence identity, suggesting that neither the overall net charge of the protein nor minor structural changes underlie the difference in redox potentials.

A common theme among the high- and low-potential Fds is the relatively large number of hydrophobic aromatic residues that surround the cluster. However, low-potential Fds typically position the cluster closer to the protein surface, with a greater likelihood of solvent influence (Fig. 2), whereas for HiPIPs the cluster is completely inaccessible to water and is surrounded by hydrophobic residues (*8*, *20*). The importance of this fact for understanding the relative $E_m$ values of Fds has been debated (*8*, *20*, *119*). In this regard, Moulis *et al.* (*123*) have studied the HiPIP from the thermophilic purple sulfur bacterium *Chromatium tepidum*, which shows optimal growth at 50°C. It was found that HiPIP from *C. vinosum* shares 74 of the 83 residues composing the primary structure of *C. tepidum* HiPIP. The most significant difference involves a stretch of eight amino acids that acts as a link between two strands of a twisted $\beta$-sheet that coordinates the 4Fe–4S cluster, and an area of extensive interaction of the cluster with the solvent. Regardless of this structural difference, these two HiPIPs show identical absorption and electron paramagnetic resonance spectra and redox potential.

Further variations in local environment can be demonstrated by the fact that Phe-83 and Phe-66 in both the *E. halophila* and the *C. vinosum* proteins are conserved; however, their side chains adopt

quite different conformations. Breiter *et al.* (*102*) proposed that the difference in side chain conformation of the above Phe may be one of many subtle factors in modulating oxidation–reduction potentials. However, the structurally similar Phe-54 in *E. vacuolata* II HiPIP did not show a conformation similar to that of the corresponding residue in *E. halophila*, and so another possible link between conformation and $E_m$ appears unsubstantiated (*113*).

### 3. *Hydrogen Bonding*

Differences in the numbers of hydrogen bonds from backbone amides to cysteine and sulfide ligands have long been believed to play a significant role in the differentiation of high- and low-potential Fds. In the case of the low-potential Fds, eight hydrogen bonds per cluster are identified between amide N–H and sulfur ligands, whereas in structurally characterized HiPIPs there are only five. The NH–S bonds are speculated to stabilize the more negatively charged reduced states (*4*, *20*, *124*). However, the comparative study of Rayment *et al.* (*114*) clearly demonstrates that such a correlation (summarized in Table IV) cannot fully explain the wide variation of $E_m$ values for this class of center. Perhaps the number of H-bond contacts better reflects other structural constraints around the cluster binding pocket, but does not influence $E_m$ strongly, per se. This conclusion is further supported by experimental solution studies. In particular, Sweeney and

TABLE IV

INFLUENCE OF HYDROGEN-BOND CONTACTS ON 4Fe–4S CLUSTER $E_m$[a]

| Protein | $E_m$ (mV) | H-bond contacts[b] |
|---|---|---|
| *Ectothiorhodospira halophila* I HiPIP | +120 | 5 |
| *Ectothiorhodspira vacuolata* II HiPIP | +150 | 5 |
| *Chromatium vinosum* HiPIP | +360 | 5 |
| *Rhodocyclus tenuis* HiPIP | +330 | 5 |
| *Clostridium pasteurianum* Fd[c] | −403 | —[d] |
| *Bacillus thermoproteolyticus* Fd[e] | −280 | 8 |
| *Peptococcus aerogenes* Fd[f] | −430 | 8 |
| *Azotobacter vinelandii* Fd I[g] | −650 | 8 |

[a] From Refs. *102*, *113*, *114*, *181*, and *182*.
[b] Number of H-bond contacts per 4Fe–4S center.
[c] Contains 2× 4Fe–S centers.
[d] Not evaluated.
[e] Contains 1× 4Fe–4S center.
[f] Contains 2× 4Fe–4S centers.
[g] Contains 1× 4Fe–4S center and 1× 3Fe–4S center.

Magliozzo (*125*) have examined the effect of deuterium substitution of exchangeable hydrogen atoms on the $E_m$ of *C. pasteurianum* Fd. Deuteration of the slowly exchangeable H atoms yielded essentially no shift in $E_m$, and so the NH–S bonds are apparently not important in the modulation of cluster reduction potential in this protein.

### C. Intermolecular Aggregation

Most HiPIPs have been assumed to function as monomers. However, the HiPIP from *Rhodospirillum salinarum* has been shown to exist as a tetramer or hexamer (*17*). Other evidence points to aggregation as a common phenomenon for HiPIPs, with possible functional implications. Dunham *et al.* interpreted EPR features observed in concentrated solutions of *C. vinosum* HiPIP as arising from dimerization (*27*), whereas *E. halophila*, *E. vacuolota*, and *R. tenuis* HiPIPs crystallize as dimers (*113*). Although the same general face is involved in this dimerization, it was noted that the orientations of protein units were distinct for each. Nevertheless, it is possible that this hydrophobic face may be involved in physiological interactions with redox partners.

## IV. Functional Roles of Residues

The preceding discussion paints a rather confusing picture of the critical factors that control cluster chemistry. Only recently, with the power of site-directed mutagenesis, have some of the functional roles of specific residues that form the cluster binding pocket been resolved. Figures 1 and 3 show that in *C. vinosum* HiPIP the iron–sulfur cluster is enclosed by several hydrophobic aromatic side chains from the C-terminal domain (residues 43–80) and a short portion of the N-terminal domain (residues 17–20) (*110*). This N-terminal sequence adopts an $\alpha$-helical conformation and accommodates a conserved tyrosine residue that lies in close proximity (3.75 Å) to the reduced cluster (Figs. 3 and 4) (*2*, *113*). The importance of these residues in mediating electron transfer and controlling cluster redox potentials has been a subject of speculation (*2*, *3*, *110*, *126*, *127*), but had not been tested. To address these questions, two groups have synthesized and expressed genes for the high-potential iron proteins from *C. vinosum* and *E. halophila* I behind the T7 *lac* promoter in a pET-21(d)(+) expression vector in *E. coli* (*128*, *129*). Such expression systems yield ~35 mg of HiPIP per liter of cell culture, while mutagenesis and iso-

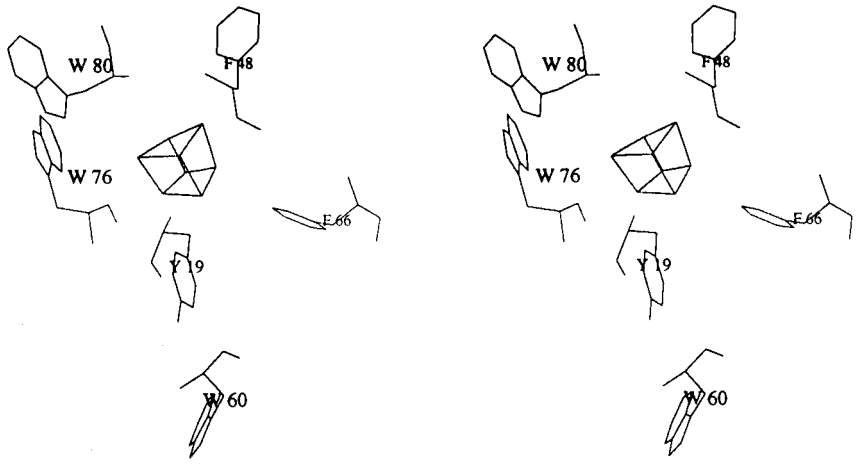


FIG. 3. Stereoview of the aromatic residues forming the hydrophobic pocket for the 4Fe–4S cluster in *Chromatium vinosum* HiPIP.

topic labeling is facile. The availability of recombinant proteins has allowed a critical assessment of the functional role of individual residues in iron–sulfur proteins by use of site-directed mutagenesis (*13*, *130–134*). Furthermore, incorporation of isotopic labels ($^{15}N$, $^{13}C$) and $^{19}F$-labeled amino acids allows the use of advanced NMR techniques (*42*, *43*, *48*, *49*, *135–137*) to explore the chemistry of the 4Fe–4S prosthetic site. These studies have contributed to the many recent advances in this area of cluster chemistry, although in some cases the

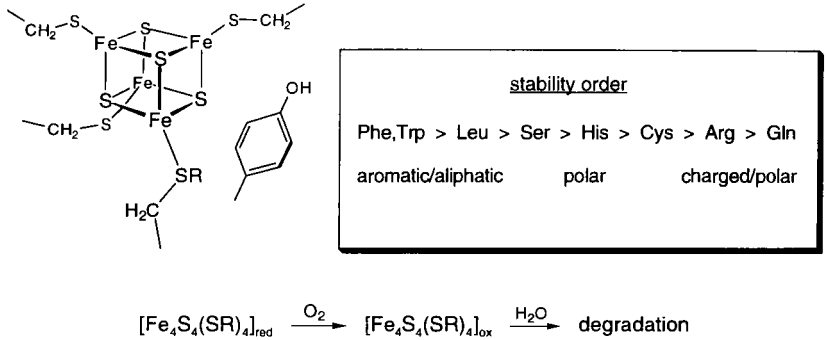


FIG. 4. Stability order for the 4Fe–4S cluster in *Chromatium vinosum* HiPIP following oxidation. A likely mechanism for the oxidative instability of the reduced protein in an aerobic environment is shown.

results have sharply contrasted with prior proposals and expectations. Subsequent discussions herein explore the chemistry of residues in the inner core as they relate to cluster stability, solvent accessibility, and redox chemistry. Unless otherwise stated, residue numbering will correspond to *C. vinosum.*

## A. Cluster Stability

### *1. Tyrosine 19*

The N-terminal sequence adopts an $\alpha$-helical conformation and accommodates a conserved tyrosine residue that lies in close proximity to the reduced cluster (Fig. 3), and has been implicated in defining the cluster potential and electron transfer pathways. In fact, excluding four cysteines, only two residues, Tyr-19 and Gly-75, are structurally conserved over the series *C. vinosum*, *E. vacuolata*, *E. halophila*, and *R. tenuis*. The conserved Gly is possibly to satisfy the steric requirements of the Tyr, which abutts the cluster. To evaluate the functional role of this key residue, a large number of mutants (Tyr-19Ser, Cys, Phe, Trp, Leu, Ile, Ala, Gln, Arg, and His) have been stably expressed in *E. coli* as holoproteins and found to be stable in the reduced form (*131*, *134*), but exhibited varying degrees of oxidative instability in the presence of dioxygen as quantitatively evaluated by direct monitoring of the change in cluster absorbance accompanying degradation (*131*). Minimal changes are observed in $E_m$ for these mutants, and this topic is addressed in more detail in Section IV,C.

*a. Oxidative Degradation of Mutants.* It has been observed that oxidized native HiPIP is unstable relative to the reduced form (although over a much longer time scale) (*138*). These mutants show the same sensitivity, but in an accelerated time frame. The relative stability of each mutant was found to vary significantly, with the aromatic Phe and Trp mutants being the most stable, and the polar Ser and Arg mutants being the least stable (Fig. 4, Table V). With the exception of the Phe and Trp mutants, oxidation by atmospheric oxygen resulted in rapid decomposition of the iron–sulfur cluster, as evidenced by the decrease in absorbance at 388 nm. Because ferricyanide oxidation also resulted in rapid cluster degradation, the oxidative instability of the cluster appears to originate from the intrinsic oxidation state of the cluster in the modified protein environment, rather than attack by reactive oxygen-derived radicals following cluster oxidation by molecular oxygen. Exclusion of dioxygen was observed to improve the stability of the mutant proteins. The aromatic residue at

TABLE V

DECAY OF FERRICYANIDE-OXIDIZED HiPIPs IN AN ANAEROBIC ENVIRONMENT[a]

| Protein | $k$ ($min^{-1}$)[b] | $t_{1/2}$ (min) |
|---|---|---|
| Native | —[c] | — |
| Tyr-19Phe,Trp | —[c] | — |
| Tyr-19Leu | $2.0 \pm 1.0 \times 10^{-2}$ | 34 |
| Tyr-19Ser | $3.7 \pm 1.2 \times 10^{-2}$ | 19 |
| Tyr-19His | $4.4 \pm 0.8 \times 10^{-2}$ | 16 |
| Tyr-19Cys | $5.1 \pm 1.2 \times 10^{-2}$ | 14 |
| Tyr-19Arg | $8.8 \pm 2.1 \times 10^{-2}$ | 8 |
| Tyr-19Gln | $54 \pm 6.3 \times 10^{-2}$ | 1.3 |

[a] Data from Ref. *131*.

[b] Measurements made at ambient temperature in 10 m*M* Tris buffer (pH 7.0).

[c] Stable on this time scale.

position 19 is therefore essential for oxidative stability of the 4Fe–4S cluster, with a minimal influence on $E_m$.

*b. Mechanism of Cluster Degradation.* Tyr-19 mutant proteins demonstrate, to varying extents, increased solvent access to the cluster pocket. This is quantitated by the determination of rate constants for $H_2O/D_2O$ exchange, measured by NMR experiments, which reflect the ability of water molecules to exchange with backbone amide protons and Trp NHs in the cluster binding pocket. (NMR methods for elucidating solvent accessibility to the cluster are described in Section IV,B.) These observations are consistent with a model in which Tyr-19 plays a critical role in preserving the structural rigidity of the polypeptide backbone through H-bonding from the phenolic OH, which lies 3.0 Å from the amide of Asn-72, and 2.7 Å from a conserved solvent molecule (*114*), to maintain a hydrophobic barrier for exclusion of water from the cluster cavity. It has been proposed that in the absence of the aromatic ring at position 19, solvent accessibility results in facile oxidation of the cluster by dissolved oxygen, with subsequent rapid hydrolysis of the $[Fe_4S_4(SR)_4]^-$ core. Such a decrease in cluster stability in the absence of a polar solvent is consistent with previous studies of model complexes that demonstrate sensitivity of the oxidized $[Fe_4S_4(SR_4]^-$ core to hydrolytic decomposition (*139–143*). The stability of such clusters is significantly improved in solvents of low polarity. Similarly, sterically encumbered, hydrophobic thiolate ligands are found to stabilize the $[Fe_4S_4(SR)_4]^-$ core (*141*, *144*).

The chemistry developed from Tyr-19 mutants is summarized in Fig. 4, and the main conclusions are as follows: (1) Tyr-19 excludes $H_2O$ from the cluster binding pocket; (2) degradation is not mediated by reactive oxygen species; and (3) cluster degradation arises through hydrolysis of the oxidized cluster. The influence of the charged residues or increased solvent access on the $E_m$ of the cluster is discussed in Section IV,C.

*c. Calorimetric Investigation of Protein Stability.* Similar trends have been observed in the stability of the homologous Tyr-12 mutants of *E. halophila* 1 HiPIP (*134*). For this protein the relative stabilities of native and mutant HiPIPs have been quantitatively evaluated by differential scanning calorimetry. The data was best fit by a three-step model (Scheme 2) that included the reversible endothermic unfolding of the polypeptide (step 1), the exothermic release of the 4Fe–4S cluster (step 2), and an irreversible transition to the final state at high temperatures (step 3).

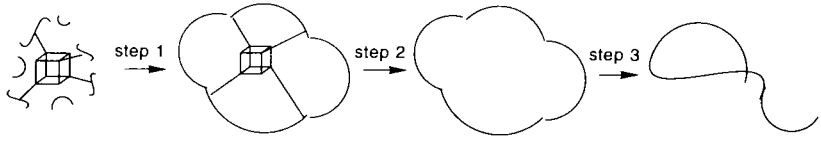


**Scheme 2**

Assuming that release of the cluster is a constant, and that the exothermic response from each of the mutants and native protein is independent of pH, the apparent destabilization energies ($\Delta\Delta H_D^{app}$) were estimated for the mutants relative to native HiPIP. Table VI summarizes pertinent data. Both changes to the side chain at position 12, and pH variations, result in destabilization of the protein. Because the packing volumes for Tyr and Phe are similar (*145*), the $\Delta T_m$ of $-12.9$°C relative to native at pH 7 reflects the importance of the hydrogen bonds, formed between the hydroxyl of Tyr-12 and both the amide side chain of Asn-14 and the backbone amide of Lys-59, to the overall structural stability of the protein. Because H bonds are estimated to contribute from 0.5 to 1.5 kcal $mol^{-1}$ to protein stability, the $\Delta\Delta G_D^{app}$ of 2.3 kcal $mol^{-1}$ for Tyr-19Phe at pH 7 is consistent with loss of two H bonds. Interestingly, the largest loss in stability was found with the Trp mutants, most likely as a result of the structural perturbations required to accommodate the larger Trp side chain.

It should be noted that the stability trend in Table VI, measured

TABLE VI

DIFFERENTIAL SCANNING CALORIMETRY DATA FOR Tyr-12 MUTANTS OF *Ectothiorhodospira halophila* I HiPIP[a]

| Protein | pH | $T_m$ (°C) | $\Delta\Delta H_D^{app}$ (kcal mol$^{-1}$)[b] | $\Delta\Delta G_D^{app}$ (kcal mol$^{-1}$)[b] |
|---|---|---|---|---|
| Native | 7.0 | 67.7 | −21.7 | −12.9 |
| | 9.0 | 66.4 | −23.0 | −12.0 |
| | 10.0 | 66.5 | −22.9 | −12.3 |
| | 10.8 | 56.7 | −33.4 | −19.6 |
| | 11.0 | 50.3 | −40.3 | — |
| Tyr-12Phe | 7.0 | 54.8 | −21.2 | — |
| | 9.0 | 54.4 | −20.7 | — |
| | 10.0 | 54.2 | −24.2 | — |
| | 10.8 | 37.1 | −29.2 | — |
| Tyr-12Trp | 7.0 | 37.4 | −23.7 | −30.3 |
| Tyr-12His | 7.0 | 42.2 | −33.3 | −25.5 |
| | 9.0 | 39.0 | −53.3 | −27.4 |

[a] Data from Ref. *134*.
[b] 1 kcal ≡ 4.2 kJ.

by relative $\Delta\Delta H_D^{app}$ values, is different from that reported in Fig. 4 for Tyr-19 mutants of HiPIP; however, in each case different properties were being measured, namely, the stability of the tertiary structure in the former and the stability of the cluster in the latter case. This is, at first, surprising because there is a strong structural homology between *C. vinosum* and *E. halophila* HiPIP, and similar stabilities might be expected. The abrupt change in $\Delta\Delta H_D^{app}$ between pH 10 and 11 most likely reflects a change in ionization state of a titratable residue. On the basis of $pK_a$ values, solvent accessibility, and structural contacts with other residues, Lys-59 is a likely candidate because this has a $pK_a$ of 10.4 and forms a salt bridge to Gln-61.

### 2. *Phenylalanines 48 and 66*

A number of point mutations of the conserved aromatic residues, phenylalanines 48 and 66 (Phe-48His,Arg and Phe-66Tyr,Asn,Cys,-Ser), in *C. vinosum* high-potential iron–sulfur protein have been examined with the aim of understanding the functional role of these residues (*130*, *146*). Both Phe-48 and Phe-66 lie in the cluster binding pocket, and Phe-66 possibly $\pi$-complexes with the cluster. Nonconservative replacements with polar residues have a minimal effect on the midpoint potential of the $[Fe_4S_4(SR)_4]^{-/2-}$ cluster, typically less than +25 mV, with a maximum change of +40 mV for Phe-66Asn (dis-

cussed more fully in Section IV,C). With the exception of the Phe-66Tyr mutant, the oxidized state is found to be unstable relative to the recombinant oxidized native protein, with regeneration of the reduced state. A likely pathway for this transformation is summarized in Scheme 3 and appears to involve degradation of the cluster in a fraction of the sample, which provides the reducing equivalents required to bring about reduction of the remainder of the sample. Some experimental observations that support this model include the observation of a transient $[Fe_3S_4(SR)_3]^{2-}$ EPR signal that is generated and then decays (but maximally constitutes only ~13% of the total sample) and the fact that >20% of the sample degrades to apoprotein, depending on the excess concentration of oxidant used.

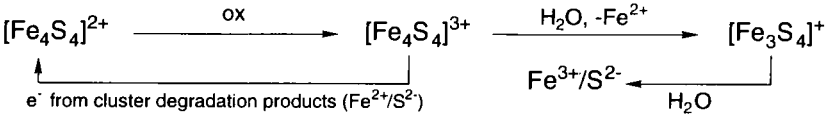


Scheme 3

This degradative reaction appears to proceed through an $[Fe_3S_4(SR)_3]^{2-}$ intermediate that is characterized by a typical EPR signature (Fig. 5) and power saturation behavior (Fig. 6), and is prompted by the increased solvent accessibility of the cluster core in the nonconservative Phe-66 mutants as evidenced by $^1H-^{15}N$ heteronuclear single quantum coherence (HSQC) NMR experiments, to be described in Section IV,B (*130*). These results are consistent with a model where, again, an important role of the aromatic residues (Fig. 3) is to protect the cluster from hydrolytic degradation in the oxidized state. In the case of Tyr-19 mutants, auto-reduction is not usually observed because the mutants are less stable and the cluster rapidly degrades as a result of increased solvent accessibility.

### *3. Cysteine 77*

The influence of oxygen ligation on 4Fe–4S cluster properties has been examined in the Cys-77Ser mutant of *C. vinosum* HiPIP (*108*, *147*, *148*). In the reduced state there is evidence for only minor perturbations to the electronic structure of the cluster, as indicated by the similar pattern of NMR chemical shifts relative to native HiPIP. In contrast, there appears to be a stronger electronic interaction between the hard O donor of the Ser ligand and the oxidized cluster; consequently the oxidized Cys-77Ser mutant shows rather dramatic

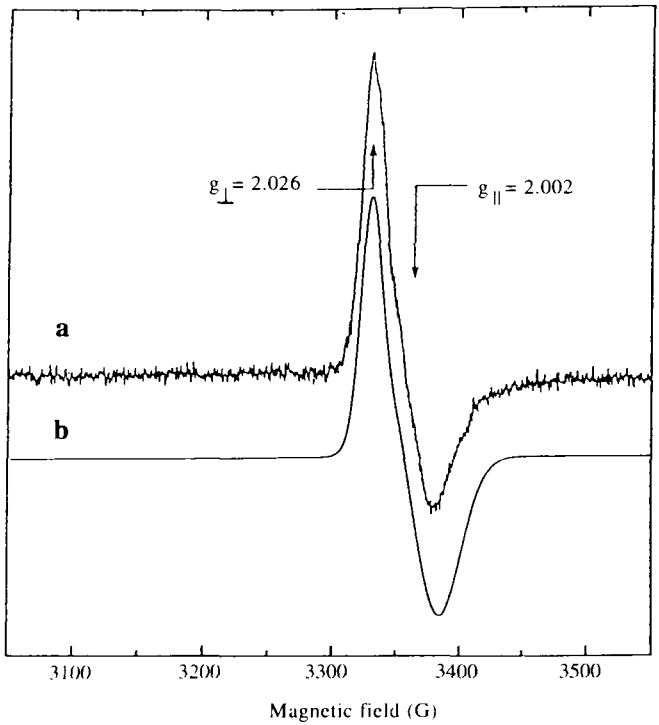


FIG. 5. (a) EPR spectrum of the intermediate formed during oxidative degradation of Phe-66Cys HiPIP. (b) Computer simulation of the spectrum. The EPR spectrum was obtained with a microwave frequency of 9.456 GHz, a modulation frequency of 100 kHz, a modulation amplitude of 1 G, a microwave power of 1.2 mW, and a temperature of 15 K (*130*).

changes in the NMR spectra, which reflect a change in electron localization on the cluster (*147*). In particular, there is a change in the pair of iron centers ascribed to the mixed-valent pair (Fig. 7). Substitution of a sulfur thiolate by an oxygen ligand does not, however, significantly perturb the $E_m$ for the $[Fe_4S_4(SR)_4]^{-/2-}$ couple; the reduction potential of Cys-77Ser decreases by only ~30 mV relative to native protein, consistent with the change from sulfur to oxygen ligation.

Most of the Cys-77Ala,Asp,Tyr mutants tested did not yield stable proteins because the ligands were either electronically or sterically incapable of binding to the vacant coordination site on iron; only the Cys-77Ser mutant resulted in formation of a stable cluster, thus we conclude that the iron center must be ligated to achieve a stable as-

| | oxidized native | | $[Fe_3S_4]^+$ intermediate | |
|---|---|---|---|---|
| | $g_\perp$ | $g_\parallel$ | $g_\perp$ | $g_\parallel$ |
| $P_{1/2}$ (mW) | 7 | 20 | 0.1 | 0.05 |

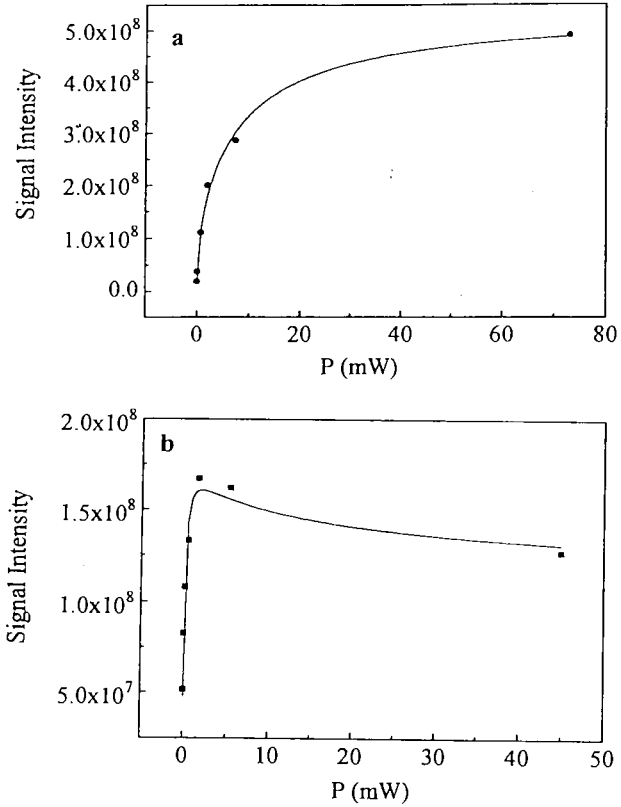


FIG. 6. Power saturation profile of (a) native and (b) $[Fe_3S_4(SR)_3]^{2-}$ intermediate forms (*130*). Saturation powers are summarized at the top of the figure.

sembly. The selection of Cys rather than Ser as a cluster ligand would appear to result more from the intrinsic stability of thiolate coordination, rather than modulation of the reduction potential.

### *4. Lessons from Model Complexes*

The general trend observed following mutation of hydrophobic residues in the cluster pocket is an increase in solvent accessibility, re-

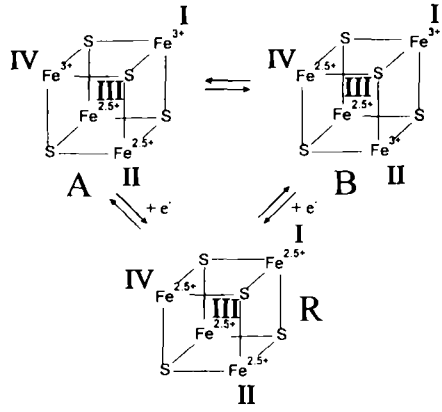


FIG. 7. Change in charge distribution over the $[Fe_4S_4(SR)_4]^-$ cluster following mutation of Cys-77 to Ser (*147*). In the reduced cluster **R**, each iron has a formal +2.5 charge. In the oxidized form the cluster equilibrates between the two states **A** and **B**. Residue 77 coordinates to iron ion IV. State **A** is favored when the harder ligand Ser binds in the Cys-77Ser mutant. (Reprinted with permission from Ref. *147*: Babini, E.; Bertini, I.; Borsari, M.; Capozzi, F.; Dikiy, A.; Eltis, L. D.; Luchinat, C. *J. Am. Chem. Soc.* **1996,** *118,* 75. Copyright 1996 American Chemical Society.)

sulting in facile oxidation of the cluster by atmospheric oxygen and subsequent rapid breakdown of the $[Fe_4S_4(SR)_4]^-$ core by water. Such a decrease in cluster stability in the presence of a polar solvent is consistent with previous studies of model complexes that demonstrate sensitivity of the oxidized $[Fe_4S_4(SR)_4]^-$ core to solvolytic decomposition (*139–143*). Cluster degradation appears to proceed by way of an $[Fe_3S_4(SR)_3]^{2-}$ center, both in the case of proteins and model complexes. There is, in fact, extensive evidence from model studies for oxidative conversion of an $[Fe_4S_4(SR)_4]^-$ core to an $[Fe_3S_4(SR)_3]^{2-}$ center, and subsequent degradation in nucleophilic solvents (*142*). In enzyme systems, oxidative conversion to an $[Fe_3S_4(SR)_3]^{2-}$ center was first reported for mammalian aconitase (*28, 83, 84, 100, 101*).

In the case of aconitase and other proteins carrying a 3Fe–4S cluster, the absence of a Cys ligand is in part responsible for the lability of the fourth iron center. Of relevance here is a modeling study by Tanaka and co-workers (*144*), who have shown that the adamantanethiolate-ligated cluster, $[Fe_4S_4(SAd)_4]^-$, exhibits extreme lability in $H_2O$/DMF (3 vol%), but found that the presence of free AdSH in $H_2O$/DMF (23 vol%) significantly enhanced its stability. The authors proposed that the hydrolysis of $[Fe_4S_4(SAd)_4]^-$ results from dissociation of the terminal ligand, followed by coordination of $H_2O$ to the cluster core; suggesting that the oxidation state of the synthetic 4Fe–4S clus-

ter can be stabilized by inhibiting dissociation of the terminal thiolate ligands from the cluster core. Strong association of the bound Cys is undoubtedly a requirement for the stability of solvent-exposed clusters.

## B. Solvent Accessibility

Solvent accessibility of native and mutant HiPIPs has been determined by multinuclear NMR methods, in particular, by use of the $^1H/^2H$ exchange rates of backbone amide protons, evaluated by $^1H-^{15}N$ HSQC experiments, and from the isotopic perturbation of $^{19}F$ chemical shifts of labeled native and mutant HiPIPs (*43*, *149*).

### *1. $^1H-^{15}N$ HSQC to Probe Backbone Amide Proton Exchange and Solvent Accessibility*

Because $^1H-^{15}N$ coupling is over one bond, the intensity of cross-peaks in a $^1H-^{15}N$ HSQC experiment does not depend on backbone conformation. This contrasts with the intensity of cross-peaks (and the magnitude of coupling constants) in the fingerprint region of a homonuclear $^1H,^1H$ correlated spectroscopy (COSY) experiment, which results from a three-bond (H–N–$C^\alpha$–H), or higher (in the case of a total correlated spectroscopy (TOCSY) experiment), correlation that will vary with a change of backbone dihedral angles (*150*). The rate of change of the intensities of $^1H-^{15}N$ cross-peaks for a lyophilized sample dissolved in $D_2O$ provides a direct measure of the accessibility of solvent to the backbone amides (*149*, *150*), and permits an evaluation of $^1H/^2H$ exchange rate constants. Such experiments are illustrated in Fig. 8 and the resulting data may be presented in a color-coded representation of the exchange regimes, as described in Ref. *149*. Experiments such as these clearly demonstrate that there is no significant difference in the $^1H/^2H$ exchange regimes observed for the reduced relative to the oxidized form of recombinant native HiPIP, and that the four cluster-binding cysteines and their neighboring residues lie in the very slow exchange region. However, the backbone amides of Tyr-19 and neighboring residues are found to lie in the slow exchange regime in the native protein, but switch to the moderate or very fast exchange regimes in the Tyr-19Leu and Tyr-19His mutant HiPIPs. This trend is consistent with the stability order indicated in Fig. 4.

### *2. $^{19}F$ NMR Parameters as a Probe of Solvent Accessibility*

Because fluorine-19 NMR resonances exhibit a strong environmental dependence, they provide a probe of redox-dependent conforma-

tional change in electron transfer proteins, and structural characterization of mutants, whereas evaluation of $H_2O/D_2O$ solvent isotope effects on $^{19}F$ chemical shifts reflects solvent accessibility to various protein domains. These experiments provide a useful complement to the $^1H$–$^2H$ exchange experiments described above (*151*, *152*). Both the chemical shift and the $T_1$ relaxation time are sensitive to interaction with the solvent. When $^{19}F$ is solvent exposed the $T_1$ relaxation times become longer and the $^{19}F$ resonance frequency shows an isotopic shift when the aqueous solvent is changed from $H_2O$ to $D_2O$ (*153*, *154*). This solvent shift should be greater than 0.1 ppm to be of significance. In general, $T_1$ measurements are less reliable than the isotopic effect as a probe of solvent accessibility for proteins that contain paramagnetic cofactors, because the paramagnetic relaxation mechanism may also reduce the relaxation time.

Fluorine-labeled analogues of *C. vinosum* high-potential iron protein have been investigated by $^{19}F$ NMR spectroscopy. By incorporation of specific fluorine-labeled amino acid residues, one can insert unique probes at well-defined locations within the protein core. The synthesis and purification of 2-, 3-, and 4-fluorophenylalanine (abbreviated 2-F-, 3-F-, and 4-F-Phe, respectively), 3-fluorotyrosine (3-F-Tyr), and 5-fluorotryptophan (5-F-Trp) derivatives of *C. vinosum* HiPIP, the assignment of $^{19}F$ NMR resonances, the measurement of longitudinal relaxation times, and the temperature dependence of $^{19}F$ and $^1H$ resonances have all been reported (*42*, *43*, *136*). These measurements were used to examine structural perturbations of mutants, the dynamics of interaction of residues with the cluster, and solvent accessibility, and as a test of the relative contribution of cross-relaxation to magnetization decay.

## C. Overview of Factors Influencing Redox Properties

### *1. Key Parameters*

Many factors have been proposed to influence cluster redox potentials and electron transfer pathways, including solvent exposure, hydrophobic effects, hydrogen bonding, electric fields from backbone amide dipoles, neighboring charges, and bonding contacts mediated by $\pi$ complexation. The ability of nature to tune the redox chemistry of biological redox cofactors is indeed well illustrated by the 4Fe–4S-cluster proteins (−650 to +450 mV) and *c*-type cytochromes (−400 to +400 mV), and has been the subject of recent reports (*155*, *156*). Even within the HiPIP family the redox potentials are tuned over a large range, from +50 to +450 mV (Table II).

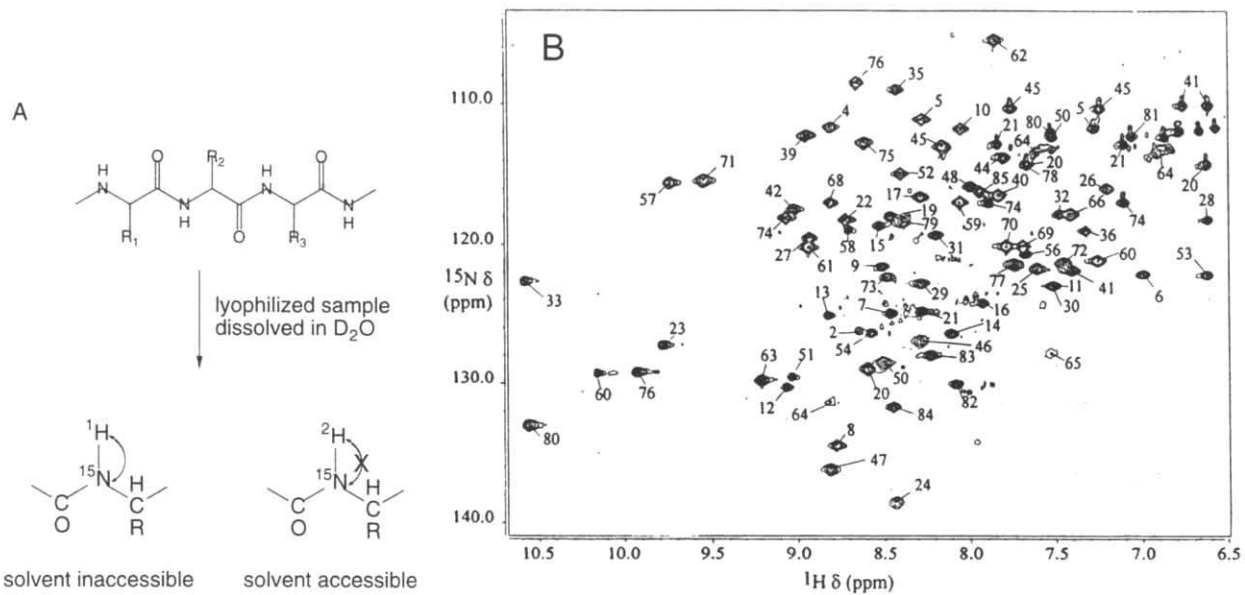


FIG. 8. Deuterium exchange of backbone amides (A) results in loss of the cross-peak intensity in $^{1}H-^{15}N$ HSQC spectra (B) and provides a probe of solvent accessibility (*149*). (C) Time course of $^{1}H-^{15}N$ HSQC spectra obtained after dissolving a lyophilized sample of *C. vinosum* HiPIP in $D_2O$ (*149*). The time (in minutes) for each spectrum is indicated in the corner of each plot. Cross-peaks disappear more rapidly for the Tyr-19Leu mutant relative to reduced native HiPIP.

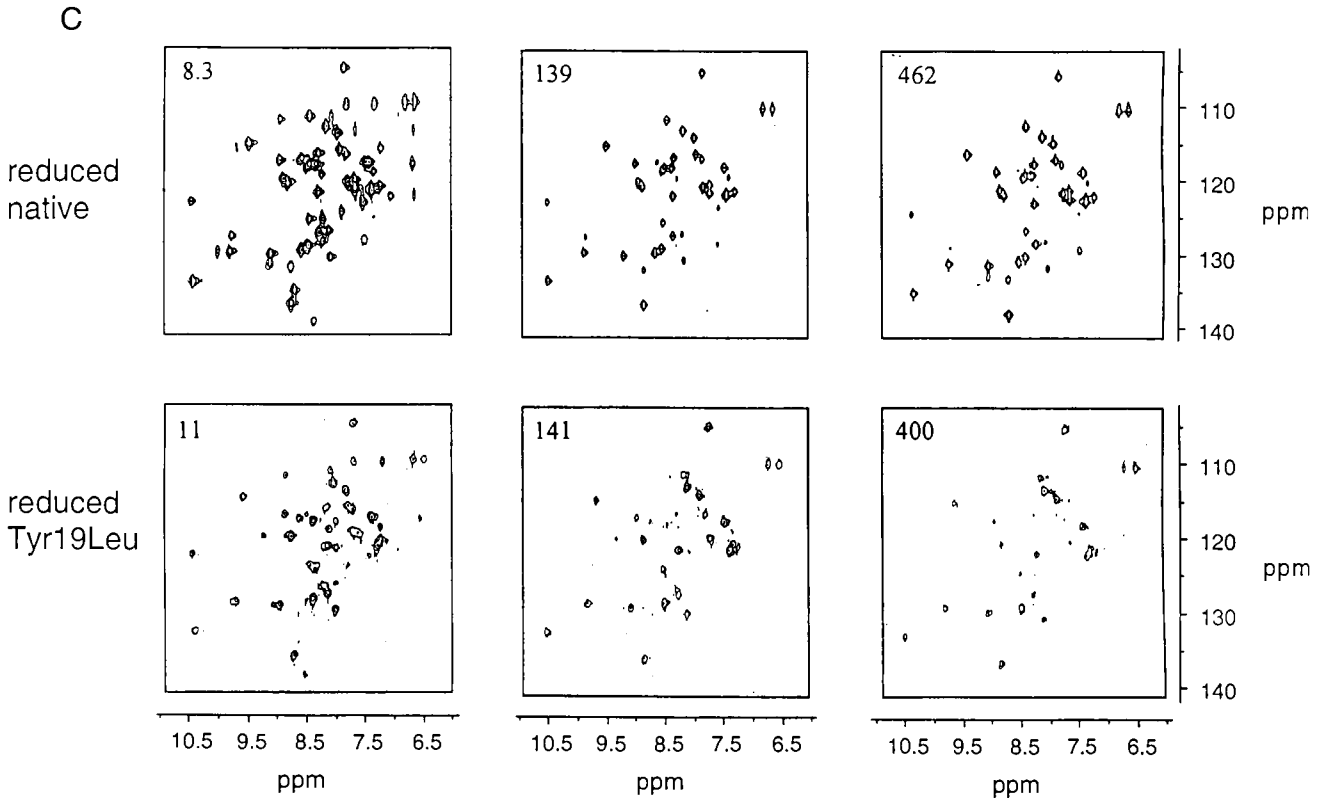


FIG. 8. *Continued*

In this section our attention is focused on the question of what factors control the relative stabilities of the $[Fe_4S_4(SR)_4]^{-/2-/3-}$ cluster states, that is, the factors underlying the three-state hypothesis of Carter (*1*), depicted earlier in Scheme 1. The cluster oxidation levels used are −1, −2, and −3; each differs by one electron and represents the net charge of the cluster, including the cysteinyl sulfur charge contributions. In terms of formal iron valences only, the −1, −2, and −3 states correspond to $[Fe_3^{3+}Fe^{2+}]$, $[Fe_2^{3+}Fe_2^{2+}]$, and $[Fe^{3+}Fe_3^{2+}]$, respectively (*61*). However, Mössbauer and NMR experiments show that the oxidized HiPIP from *E. halophila* has two iron(III) ions and one mixed-valence pair (*61*, *63*, *64*, *66*, *157*). On the basis of Mössbauer spectroscopy of *C. vinosum* (*63*, *66*, *67*) and *E. halophila* (iso II) HiPIPs (*62*), the presence of an iron(III) pair and a mixed-valence pair in the cluster is increasingly seen as a general feature of all oxidized HiPIPs, although it is unknown whether this electronic distribution is relevant for the function of the proteins. After reduction, the ferric center is localized at one site.

HiPIP can be reduced to the normally unobtainable $[Fe_4S_4(SR)_4]^{3-}$ oxidation level (superreduction), either by pulse radiolysis (*97*) or by dithionite after partial unfolding in 80% $Me_2SO$ (*158*). The structural features of the protein that underlie the thermodynamic barrier for superreduction of native HiPIP remain uncertain. Nevertheless, it has been suggested that exposure of the cluster to solvent may stabilize the reduced $[Fe_4S_4(SR)_4]^{3-}$ state. Similarly, Kamen and co-workers (*159*) reported the amino acid sequence of a HiPIP with the highest known redox potential (+450 mV) from *Rhodopila globiformis*. Based on sequence alignment with other known HiPIPs, they suggested that the very positive potential might be attributed to a more hydrophobic environment for the 4Fe–4S cluster in this protein (*159*).

### 2. *Electrostatic Influence*

Bertini and co-workers (*160*) have tried to rationalize the reduction potentials within the series of HiPIPs by quantitatively assessing the electrostatic contributions from surface-charged residues, dipolar contributions from polar residues, and solvent dipoles and polarizabilities, to the energy of the cluster. A correlation with reduction potential was found only for the net charge of the protein in the absence of other factors; however, this work does not explain the significant change in $E_m$ when comparing high- and low-potential Fds.

Backes *et al.* (*20*) and Krishnamoorthi *et al.* (*44*) suggested that the polarity of cluster environment and ability to delocalize electrons by the amino acid residues around the cluster also contribute to the posi-

tive potentials of HiPIPs. The influence of surface charges on redox potentials of HiPIPs from *R. globiformis*, *C. vinosum*, *R. gelatinosus*, *E. vacuolata* (I and II), and *E. halophila* (I and II) has been evaluated by Luchinat *et al.* using differential pulse voltammetry (*161*). The authors proposed that the peptide charge, ranging from −13 to +5, controls the redox potentials (*161*), whereas a decrease in reduction potential with pH was observed in the pH range where deprotonation of the imidazolium nitrogen of histidine residues occurs. It was suggested that surface charges may be capable of influencing the cluster potential in spite of the known quenching of electrostatic interaction by solvents.

Heering *et al.* (*162*) have used direct electrochemical measurements to study HiPIPs from various sources (*E. vacuolata* I and II, *C. vinosum*, *R. gelatinosus*, *R. tenuis*, *R. globiformis*, and *R. salinarum*). In contrast to Luchinat *et al.* (*161*), these researchers found no significant pH dependence of $E_m$ for most HiPIPs, with the exception of *C. vinosum* and *R. gelatinosus* HiPIPs (maximum slopes of −20 mV/pH unit). These researchers also divided the HiPIPs into two groups based on sequence alignment, optical spectra, overall charges, and the redox thermodynamics. First, *Chromatium*-like HiPIPs with redox potentials between 300 and 350 mV were proposed to be dominated by solvent effects; however, this is not substantiated by studies of mutant HiPIPs (*155*). Second, *Ectothiorhodospira*-like HiPIPs with potentials between 50 and 450 mV were proposed to depend on both the overall charge of the peptide and solvation; however, the evidence for this generalization is weak.

Clearly there has been substantial confusion on this issue, with many hypotheses concerning the factors that control cluster redox properties (*113*, *160*, *163*, *164*). It is only since the availability of expression systems, which allow analysis by site-directed mutagenesis, that these ideas have been open to experimental testing. In particular, the roles of key aromatic core residues in regulating the reduction potential, the enthalpy and entropy of reduction for the prosthetic $[Fe_4S_4(SR)_4]^{-/2-}$ cluster, and the self-exchange rate constants for electron transfer reactions of *C. vinosum* high-potential iron protein (HiPIP) have been directly addressed by a combination of site-directed mutagenesis, high-field NMR (EXSY) experiments, and variable-temperature spectrochemical redox titration measurements (*155*). The results of mutagenesis experiments have thus far emphasized that most of the factors previously speculated to control cluster chemistry actually play a negligible role in defining the reduction potential of the 4Fe–4S center (*134*, *155*). Surface charge may play a

minor role in defining the midpoint potential ($E_m$) (*161*); however, the ability to delocalize charge over amino acid residues, and the polarity of the cluster environment, appear to be of lesser importance (*113*, *155*). These issues are of general relevance for understanding the mechanisms employed by proteins for modulating the chemistry of protein-bound redox cofactors.

### 3. *Comparison of Thermodynamic Parameters*

Because the enthalpies and entropies of metalloprotein electron transfer processes are influenced by changes in protein conformation and solvation, as well as by other structural and medium effects (*5*, *165*, *166*), comparison of these parameters over a range of HiPIPs differing by single-point mutations affords considerable insight into the factors underlying cluster redox chemistry.

Few reports of the temperature dependence of 4Fe–4S cluster potentials have appeared in the literature. With the exception of a small number of *c*-type cytochromes, the enthalpic component is typically found to be negative for the available data on heme proteins and 4Fe–4S proteins, reflecting favorable bonding changes on reduction. For HiPIPs, the $\Delta H$ values typically lie within 4 to 5 kcal mol$^{-1}$ of each other (Table VII), which is consistent with their similar $E_m$ values and the importance of the enthalpy term in defining the free en-

TABLE VII

SUMMARY OF 4Fe–4S CLUSTER REDOX PARAMETERS FOR SELECTED MUTANT *Chromatium vinosum* HiPIPs[a]

| Protein | $E_m$ (mV) | $\Delta H$ (kcal mol$^{-1}$) | $\Delta S$ (cal K$^{-1}$ mol$^{-1}$) | $k_{ex}$ ($\times 10^{-3}$ $M^{-1}$ sec$^{-1}$) |
|---|---|---|---|---|
| Native | 345 | −32.2 | −81.4 | 14.5 |
| Cys-77Ser | 315 | −19.4 | −40.7 | — |
| Tyr-19Trp | 372 | −30.4 | −73.2 | — |
| Tyr-19Leu | 370 | −25.0 | −55.4 | 24.5 |
| Tyr-19His | 348 | −26.4 | −61.8 | — |
| Phe-66Tyr | 356 | −25.0 | −56.2 | — |
| Phe-66Cys | 361 | −27.1 | −63.1 | — |
| Phe-66Ser | 368 | −25.4 | −56.6 | 13.3 |
| Phe-66Asn | 392 | −25.1 | −54.0 | — |
| Phe-48His | 360 | −25.3 | −57.1 | 10.0 |
| Phe-48Arg | 368 | −26.0 | −59.3 | 5.0 |

[a] Data from Ref. *155*. All measurements are at 25°C; standard deviations are as follows: $E_m \pm 7$ mV; $\Delta H \pm 2$ kcal mol$^{-1}$; $\Delta S \pm 5$ cal K$^{-1}$ mol$^{-1}$. Errors in these measured rate constants ($k_{ex}$) are on the order of ±20%.

ergy for reduction. The enthalpy changes are usually more negative for the $[Fe_4S_4(SR)_4]^{-/2-}$ couple than for the $Fe^{3+/2+}$ heme couple in cytochromes (*156*), presumably as a result of favorable interactions between the cluster and the polypeptide, including coordination from four cysteine residues and favorable interactions with aromatic rings.

As an exception to the above-noted trend, the reduction enthalpies and entropies for Cys-77Ser differ markedly from native (Table VII), although the $\Delta G$ values are similar. Such an isoequilibrium relationship implies that the mutant differs from the native only with regard to the electronic properties of the cluster, with no significant structural perturbation of the surrounding peptide.

Native HiPIP shows the most negative enthalpy and entropy change. Mutants that result in either increased solvent access to the cluster, or a change from sulfur to oxygen donor ligands (such as Cys-77Ser), show enthalpy and entropy changes that are less negative relative to recombinant native HiPIP (Table VII) (*155*). These proteins do not show a substantive change in $E_m$ because the favorable entropy change is offset by a less favorable change in the reaction enthalpy. This is analogous to the situation observed for cytochromes with positive $E_m$ values as described by Bertrand *et al.* (*156*).

Asso *et al.* (*23*) have reported on the redox characteristics of ferredoxins I and II from *Desulfovibrio vulgaris* Miyazaki. For the $[Fe_4S_4(SR)_4]^{2-/3-}$ couple in Fd II, $\Delta H = +2.3$ kcal mol$^{-1}$ (+9.65 kJ mol$^{-1}$) and $\Delta S = -24.6$ cal K$^{-1}$ mol$^{-1}$ ($-103$ J K$^{-1}$ mol$^{-1}$), which demonstrates that the 760-mV difference in potential for these two clusters arises from enthalpic effects. Low-potential clusters in Fds tend to lie closer to the protein surface and are more solvent exposed; however, the available results on HiPIP mutants suggest that the difference in $\Delta H$ terms observed for the Fd may not arise from either solvent exposure or a local variation in side chain identity. However, the role of solvent may be different for HiPIPs and Fds, which employ different redox couples.

### 4. *Influence of Solvent on $E_m$*

The influence of varying solvent dielectric on the reduction potentials has been examined by Blonk *et al.* (*143*) for the cluster series $[Fe_4S_4(SR)_4]$. When R = Ph a minimal variation in $E_m$ was observed for both the high- and low-potential couples. For example, in nitrobenzene ($\varepsilon = 35.7$) $E_m = -0.33$ V, but in dichloromethane ($\varepsilon = 9.1$) $E_m = -0.32$ V for the high-potential couple. Also, when R = $^t$Bu, $E_m = -0.65$ V in dichloromethane and $-0.70$ V in *N*,*N*-dimethylformamide ($\varepsilon = 37.6$). Similar minimal variations in $E_m$ values were observed for

the low-potential redox couple. This is consistent with the observations made for the mutant HiPIPs, and seems to indicate that the lack of sensitivity of the 4Fe–4S cluster potentials to solvent is an effect that is neither limited to, nor a result of, the presence of a protein matrix.

Heering *et al.* (*162*) have argued that HiPIPs may be considered to fall into two classes, one with an $E_m$ that is independent of the total charge and centered around 336 mV, and one with an $E_m$ that is dependent on the total charge. After subtraction of the contribution from the overall charge it was proposed that the remaining part of the potential reflected variations of polarity and solvation in the local cluster environment. However, the results of studies on mutant proteins indicate no clear role for changes in the polarity of residues neighboring the cluster, and provide a clear indication that solvation is not a critical factor for HiPIPs. The results of mutational studies do not support any significant role in the definition of cluster potential (*147*, *148*, *155*). Rather, these residues appear to inhibit solvent access to the cluster pocket that can result in hydrolytic degradation of the $[Fe_4S_4(SR)_4]^-$ center.

### 5. *Self-Exchange Rates for Native and Mutant HiPIP*

The electron self-exchange transfer rate constants for native and mutant HiPIPs have been estimated using $^1H$ 2D EXSY methods (Fig. 9) (*155*). Although the net charge of the peptide chain is −3 at pH 7.0 (*126*, *167*), it has been previously noted that the redox kinetics of *C. vinosum* HiPIP do not depend on the ionic strength of the solvent, most likely reflecting the self-aggregation of HiPIPs through a hydrophobic face, in a manner consistent with other crystallographically defined HiPIP dimers (*113*). However, an increase in self-exchange rate constants with decreasing pH has previously been observed for *C. vinosum* HiPIP (*126*), and so it is likely that neutralization of charged residues at the binding interface is required for electrostatic stabilization.

Aromatic side chains surrounding the cluster have long been believed to mediate electron transfer reactions, both self-exchange reactions and electron transfer with other redox partners. On the basis of crystallographic results, Carter *et al.* (*1*) have suggested that Tyr-19 is a critical residue for mediating electron transfer, whereas Bertini *et al.* (*73*) have proposed Phe-48 as a mediator of electron transfer in the self-exchange reaction of the HiPIP from *E. vacuolata*. In early studies of oxidation–reduction chemistry of HiPIP with nonphysiological reactants, Mizrahi and co-workers (*126*) proposed several charge-

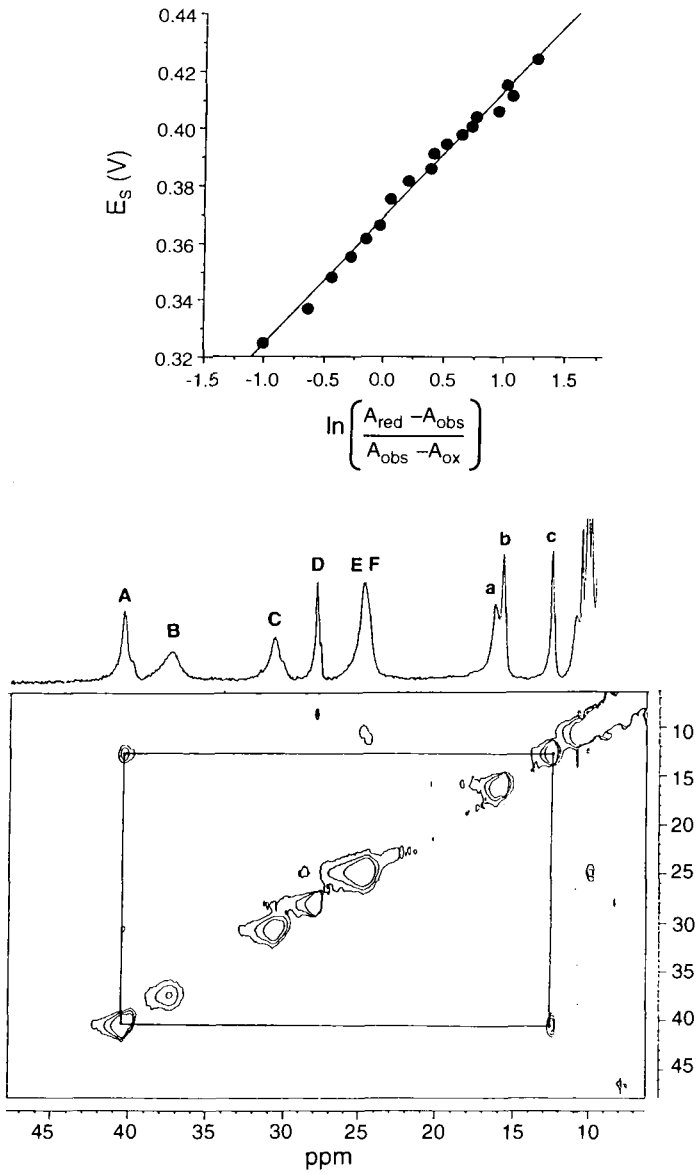


FIG. 9. (Top) Evaluation of midpoint potentials by spectrochemical titration experiments. $E_S$ is the solution potential and the $A$ values refer to the absorbances of the species. (Bottom) EXSY spectrum to evaluate electron-exchange rates. Uppercase letters denote resonances for the oxidized HiPIP, and lowercase letters indicate the reduced protein. Cross-peaks derive from the exchange of magnetization between the same proton as it switches between the oxidized and reduced protein states.

relay pathways involving Phe-48, Phe-66, and Trp-76 residues. In fact, all of these aromatic residues are widely conserved in the HiPIP family (Table VIII). However, experimental results demonstrate that, relative to native HiPIP, the exchange rates for the mutant proteins differ by no more than a factor of two. These observations are consistent with the pathway approach of Beratan *et al.* that tends to emphasize $\sigma$-bonding pathways in mediating electron transfer through a protein framework (*168*). A critical appraisal of the available experimental data, particularly for mutant proteins, suggests that the role of aromatic core residues is to prevent solvent access that might compromise the stability of the oxidized cluster, rather than to mediate cluster redox potentials or electron transfer (*119*).

The conclusion from these studies is that neither specific aromatic amino acid side chains nor solvent accessibility appear to play a major role in defining the reduction potentials or electron transfer properties of the cluster in high-potential iron proteins. The role of the aromatic core is to maintain a hydrophobic barrier to solvent water and inhibit oxidation and hydrolytic degradation of the cluster.

### 6. *Dipole Contributions to $E_m$*

Warshel and collaborators (*4*, *169*) have investigated the control mechanism for the redox potential of an Fe–S cluster by its protein

TABLE VIII

CONSERVED RESIDUES AROUND THE 4Fe–4S CORE IN SEVERAL HiPIPs

| HiPIP[a] | 17 | 19 | 48 | 49 | 60 | 65 | 66 | 68 | 71 | 75 | 76 | 80 |
|---|---|---|---|---|---|---|---|---|---|---|---|---|
| *Chromatium vinosum* | Leu | Tyr | Phe | Met | Trp | Leu | Phe | Gly | Ile | Gly | Trp | Trp |
| *Thiocapsa pfennigii* | Leu | Tyr | Phe | Ile | Trp | Leu | Tyr | Gly | Val | Gly | Trp | Trp |
| *Rhodocyclus gelatinosus* | Leu | Tyr | Leu | Phe | — | Leu | Phe | Gly | Val | Gly | Trp | Trp |
| *Rhodocyclus tenuis* | Phe | Tyr | Gln | Phe | Ala | Val | Ile | Gly | Ile | Gly | Tyr | Phe |
| *Ectothiorhodospira halophila* I | His | Tyr | Phe | Trp | Trp | Val | His | Asp | Val | Gly | Trp | Tyr |
| *Ectothiorhodospira halophila* II | His | Tyr | Phe | Trp | Trp | Val | His | Asp | Val | Gly | Trp | Tyr |
| *Ectothiorhodospira vacuolata* I | Leu | Tyr | Leu | Trp | Trp | Val | Phe | Asn | Val | Gly | Trp | Tyr |
| *Ectothiorhodospira vacuolata* II | Leu | Tyr | Leu | Trp | Trp | Val | Phe | Gly | Val | Gly | Trp | Trp |

[a] Numbering refers to *C. vinosum*.

environment, by examining the variation in the midpoint potential of the 4Fe–4S clusters of several structurally well-characterized proteins, *Azotobacter vinelandii* ferredoxin (AvFd I), *Peptococcus aerogenes* ferredoxin (PaFd), *Bacillus thermoproteolyticus* ferredoxin (BtFd), and *C. vinosum* HiPIP (CvHiPIP). By using the "protein dipoles Langevin dipoles" (PDLD) approach (*170, 171*), these researchers were able to model the protein control of the 4Fe–4S cluster redox potentials (Figs. 10 and 11). This microscopic electrostatic model includes both protein and solvent water. Langen *et al.* (*4*) have reported that the total differential solvation energies are substantially reduced in BtFd, PaFd, and AvFd I; in contrast, in *C. vinosum* HiPIP very little change occurs. These calculations demonstrated a critical role for the orientation of amide groups in the neighborhood of a cluster in tuning its reduction potential. These amides are not necessarily those involved in H-bonding to the cluster. The large differences between the potentials of the 4Fe–4S clusters of PaFd, AvFd I, and CvHiPIP were modeled and attributed principally to the different con-

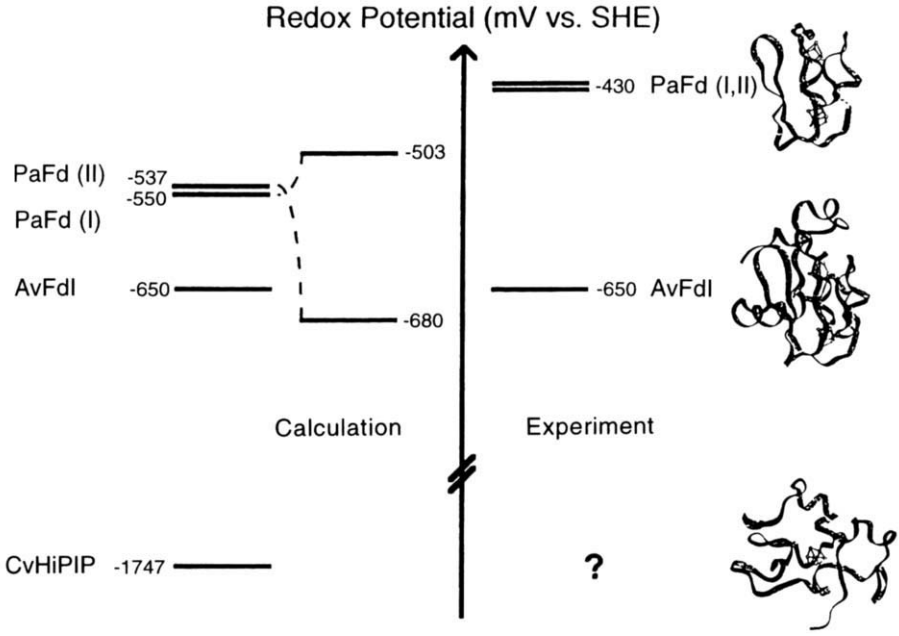


FIG. 10. Theoretical calculation of $E_m$ for the $[Fe_4S_4(SR)_4]^{2-/3-}$ redox couple in representative high- and low-potential ferredoxins. (Reprinted with permission from Ref. *169.* Jensen, G. M.; Warshel, A.; Stephens, P. J. *Biochemistry* **1994,** *33,* 10911. Copyright 1994 American Chemical Society.)

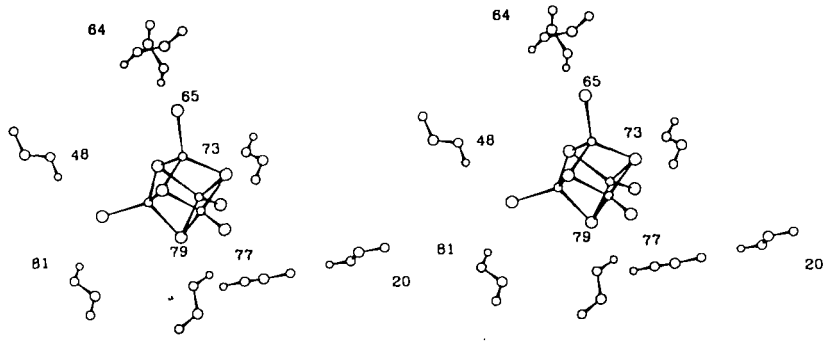


FIG. 11. Stereoview showing the orientations of amide dipoles around the cluster in *Chromatium vinosum* HiPIP. (Reproduced with permission from Ref. *169*: Jensen, G. M.; Warshel, A.; Stephens, P. J. *Biochemistry* **1994,** *33,* 10911. Copyright 1994 American Chemical Society.)

figurations of main-chain amide groups near the clusters. Also, for the two Fds, the water contribution to the redox potentials of AvFd I and PaFd, which show strong structural homology, the solvent plays an important role in establishing the trend in redox potentials. In fact, these two proteins appear to have significantly different extents of water penetration to the cluster, and solvent dipoles close to the cluster in PaFd are an important contribution to its higher potential.

In general, the differences in the oxidation levels used by the HiPIPs, in contrast to the low-potential ferredoxins, are thought to be principally due to differences in local amide dipoles, the more hydrophobic environment of the 4Fe–4S cluster, and fewer hydrogen bonds (*20*).

## V. Final Comments and Perspectives

It is clear that there have been many recent and significant advances in the understanding of iron–sulfur cluster biochemistry, and HiPIPs in particular. Many issues relating to function and the role of residues in defining $E_m$ and $k_{ex}$ have been resolved. It seems likely that future research on these proteins will focus on the still unresolved issues of cluster assembly *in vivo*, and the chemistry of nontraditional iron–sulfur proteins such as those described in Table I. In particular, the issue of how a protein environment defines the chemical role of the cluster will become increasingly clear as a result of the growing number of recombinant proteins that are accessible to analysis following site-directed mutagenesis.

## References


1. Carter, C. W. *in* "Iron-Sulfur Proteins"; Lovenberg, W., Ed.; Academic Press: NY, 1977; Vol. 3, pp. 157–204.
2. Przysieck, C. T.; Meyer, T. E.; Cusanovich, M. A. *Biochemistry* **1985,** *24,* 2524.
3. Packer, E. L.; Sternlicht, H.; Rabinowitz, J. C. *Proc. Natl. Acad. Sci. U.S.A.* **1972,** *69,* 3278.
4. Langen, R.; Jensen, G. M.; Jacob, U.; Stephens, P. J.; Warshel, A. *J. Biol. Chem.* **1992,** *267,* 25625.
5. Taniguchi, V. T.; Sailasuta-Scott, N.; Anson, F. C.; Grey, H. B. *Pure Appl. Chem.* **1980,** *52,* 2275.
6. Adzamli, I. K.; Davies, D. M.; Stanley, C. S.; Sykes, A. G. *J. Am. Chem. Soc.* **1981,** *103,* 5543.
7. Cusanovich, M. A. *Int. Symp. Interact. Iron Proteins Oxygen Electron Transp.* **1982,** 365.
8. Orme-Johnson, N. R.; Mims, W. B.; Orme-Johnson, W. H.; Bartsch, R. G.; Cusanovich, M. A.; Peisach, J. *Biochim. Biophys. Acta* **1983,** *748,* 68.
9. Augustin, M. A.; Chapman, S. K.; Davies, D. M.; Watson, A. D.; Sykes, A. G. *J. Inorg. Chem.* **1984,** *20,* 281.
10. Przysiecki, C. T.; Meyer, T. E.; Cusanovich, M. A. *Biochemistry* **1985,** *24,* 2542.
11. Bhattacharyya, A. K.; Meyer, T. E.; Cusanovich, M. A.; Tollin, G. *Biochemistry* **1987,** *26,* 758.
12. Ueyama, N.; Terakawa, T.; Sugawara, T.; Fuji, M.; Nakamura, A. *Chem. Lett.* **1984,** *8,* 1287.
13. Iismaa, S.E.; Vazquez, A. E.; Jensen, G. M.; Stephens, P. J.; Butt, J. N.; Armstrong, F. A.; Burgess, B. K. *J. Biol. Chem.* **1991,** *266,* 21563.
14. Ueyama, N.; Terakawa, T.; Nakata, N.; Nakamura, A. *J. Am. Chem. Soc.* **1983,** *105,* 7098.
15. Hartshorn, R. T.; Lim, M. C.; Sykes, A. G. *Inorg. Chem.* **1988,** *27,* 4603.
16. Ohno, R.; Ueyama, N.; Nakamura, A. *Inorg. Chim. Acta* **1990,** *169,* 253.
17. Meyer, T. E. F. J.; Bartsch, R. G.; Tollin, D.; Cusanovich, M. A. *Biochim. Biophys. Acta* **1990,** *1017,* 118.
18. Kuznetsov, B. A.; Shumakovich, G. P.; Mutuskin, A. A.; Mazhorova, L. E. *Dokl. Akad. Nauk SSSR* **1990,** *312,* 1244.
19. Jackman, M. P.; Lim, M. C.; Sykes, A. G.; Salmon, G. A. *J. Chem. Soc., Dalton Trans* **1988,** *11,* 2843.
20. Backes, G.; Mino, Y.; Loehr, T. M.; Meyer, T. E.; Cusanovich, M. A.; Sweeney, W. V.; Adman, E. T.; Sanders-Loehr, J. *J. Am. Chem. Soc.* **1991,** *113,* 2055.
21. Hochkoeppler, A.; Zannoni, D.; Ciurli, S.; Meyer, T. E.; Cusanovich, M. A.; Tollin, G. *Proc. Natl. Acad. Sci. U.S.A.* **1996,** *93,* 6998.
22. Loehr, T. M. *J. Raman Spectrosc.* **1992,** *23,* 531.
23. Asso, M.; Mbarki, O.; Guigliarelli, B.; Yagi, T.; Bertrand, B. *Biochem. Biophys. Res. Commun.* **1995,** *211,* 198.
24. Banci, L.; Bertini, I.; Ferretti, S.; Luchinat, C.; Piccioli, M. *J. Mol. Struct.* **1993,** *292,* 207.
25. Bertini, I.; Ciurli, S.; Dikiy, A.; Luchinat, C. *J. Am. Chem. Soc.* **1993,** *115,* 12020.
26. Cavazza, C.; Guigliarelli, B.; Bertrand, P.; Bruschi, M. *FEMS Microbiol. Lett.* **1995,** *130,* 193.
27. Dunham, W. R.; Hagen, W. R.; Fee, J. A.; Sands, R. H.; Dunbar, J. B.; Humblet, C. *Biochim. Biophys. Acta* **1991,** *1079,* 253.
28. Emptage, M. H.; Kent, T. A.; Kennedy, M. C.; Beinert, H.; Munck, E. *Proc. Natl. Acad. Sci. U.S.A.* **1988,** *80,* 4674.

29. Gayda, J. P.; Bertrand, P.; More, C.; Le Gall, J.; Cammack, R. C. *Biochem. Biophys. Res. Commun.* **1981,** *99,* 1265.
30. Gloux, J.; Gloux, P.; Lamotte, B.; Mouesca, J.-M.; Rius, G. *J. Am. Chem. Soc.* **1994,** *116,* 1953.
31. Heering, H. A.; Bulsink, Y. B. M.; Hagen, W. R.; Meyer, T. E. *Eur. J. Biochem.* **1995,** *232,* 811.
32. Hu, Z.; Jollie, D.; Burgess, B. K.; Stephens, P. J.; Munck, E. *Biochemistry* **1994,** *33,* 14475.
33. Papaefthymiou, V.; Millar, M. M.; Muenck, E. *Inorg. Chem.* **1986,** *25,* 3010.
34. Peisach, J.; Beinert, H.; Emptage, M. H.; Mims, W. B.; Fee, J. A.; Orme-Johnson, W. H.; Redina, A. R.; Orme-Johnson, N. B. *J. Biol. Chem.* **1983,** *258,* 13014.
35. Banci, L.; Bertini, I.; Briganti, F.; Luchinat, C.; Scozzafava, A.; Oliver, M. V. *Inorg. Chem.* **1991,** *30,* 4517.
36. Banci, L.; Bertini, I.; Carloni, P.; Luchinat, C.; Orioli, P. L. *J. Am. Chem. Soc.* **1992,** *114,* 10684.
37. Banci, L.; Bertini, I.; Carloni, P.; Luchinat, C.; Orioli, P. L. *J. Am. Chem. Soc.* **1992,** *114,* 10683.
38. Banci, L.; Pieratelli, R. *NATO ASI, Ser. C* **1995,** *457,* 281.
39. Sola, M.; Cowan, J. A.; Gray, H. B. *Biochemistry* **1989,** *28-12,* 5261.
40. Sola, M.; Cowan, J. A.; Gray, H. B. *J. Am. Chem. Soc.* **1989,** *111,* 6627.
41. Rueterjans, H.; Messori, L.; Ohlenschlaeger, O.; Briganti, F.; Bertini, I. *Appl. Magn. Reson.* **1993,** *4,* 477.
42. Li, D.; Soriano, A.; Cowan, J. A. *Inorg. Chem.* **1996,** *35,* 1980.
43. Li, D.; Agarwal, A.; Cowan, J. A. *Book of Abstracts, 210th ACS National Meeting* **1995,** *Issue Pt. 1,* INOR-674.
44. Krichnamoorthi, R.; Cusanovich, M. A; Meyer, T. E.; Przysiecki, C. T. *Eur. J. Biochem.* **1989,** *181,* 81.
45. Ciurli, S.; Cremonini, A.; Kofod, P.; Luchinat, C. *Eur. J. Biochem.* **1996,** *236,* 405.
46. Ciurli, S.; Luchinat, C.; Scozzafava, A. *Top. Mol. Organ. Eng.* **1994,** *11,* 143.
47. Cheng, H.; Markley, J. L. *Annu. Rev. Biophys. Biomol. Struct.* **1995,** *24,* 209.
48. Bertini, I.; Eltis, L. D.; Felli, I. C.; Kastrau, D. H. W.; Luchinat, C.; Piccioli, M. *Chem Eur. J.* **1996,** *1,* 598.
49. Bertini, I.; Dikiy, A.; Kastrau, D. H. W.; Luchinat, C.; Sompornpisut, P. *Biochemistry* **1995,** *34,* 9851.
50. Bertini, I.; Capozzi, F.; Luchinat, C.; Piccioli, M.; Vicens Oliver, M. *Inorg. Chim. Acta* **1992,** *198-200,* 483.
51. Bertini, I.; Capozzi, F.; Ciurli, S.; Luchinat, C.; Messori, L.; Piccioli, M. *J. Am. Chem. Soc.* **1992,** *114,* 3332.
52. Banci, L.; Bertini, I.; Dikiy, A.; Kastrau, D. H. W.; Luchinat, C.; Sompornpisut, P. *Biochemistry* **1995,** *34,* 206.
53. Banci, L.; Bertini, I.; Luchinat, C.; Messori, L.; Torano, P. *Appl. Magn. Reson.* **1993,** *4,* 461.
54. Bertini, I.; Capozzi, F.; Luchinat, C.; Piccioli, M. *Eur. J. Biochem.* **1993,** *212,* 69.
55. (a) Blondin, G.; Girerd, J.-J. *J. Biol. Inorg. Chem.* **1996,** *1,* 170; (b) Krockel, M.; Grodzicki, M.; Papaefthymiou, M.; Trautwein, A. X.; Kostikas, A. *ibid.* 173; (c) Noodleman, L.; Case, D. A.; Mouesca, J.-M.; Lamotte, B. *ibid.* 177; (d) Bertini, I.; Luchinnat, C. *ibid.* 183; (e) Belinsky, M. I. *ibid.* 186.
56. Aizman, A.; Case, D. A. *J. Am. Chem. Soc.* **1982,** *104,* 3269.
57. Mouesca, J.-M.; Noodleman, L.; Case, D. A. *J. Quant. Chem., Quant. Biol. Symp.* **1995,** *22,* 95.

58. Noodleman, L. *Inorg. Chem.* **1988,** *27,* 3677.
59. Antanaitis, B. C.; Moss, T. H. *Biochim. Biophys. Acta* **1975,** *405,* 262.
60. Cerdonio, M.; Wang, R.-H.; Rawlings, J.; Gray, H. B. *J. Am. Chem. Soc.* **1974,** *96,* 6534.
61. Herskovitz, T.; Averill, B. A.; Holm, R. H.; Ibers, J. A.; Phillips, W. D.; Weiher, J. F. *Proc. Natl. Acad. Sci. U.S.A.* **1972,** *69,* 2437.
62. Bertini, I.; Campos, A. P.; Luchinat, C.; Teixeira, M. *J. Inorg. Biochem.* **1993,** *52,* 227.
63. Dickson, D. P. E.; Johnson, C. E.; Cammack, R.; Evans, M. C. W.; Hall, D. O.; Rao, K. K. *Biochem. J.* **1974,** *139,* 105.
64. Middleton, P.; Dickson, D. P. E.; Johnson, C. E.; Rush, J. D. *Eur. J. Biochem.* **1980,** *104,* 289.
65. Dickson, D. P. E.; Johnson, C. E.; Middleton, P.; Rush, J. D.; Cammack, R.; Hall, D. O.; Mullinger, R. N.; Rao, K. K. *J. Phys. (Paris), Colloq.* **1976,** 171.
66. Dickson, D. P. E.; Cammack, R. *Biochem. J.* **1974,** *143,* 763.
67. Moss, T. H.; Bearden, A. J.; Bartsch, R. G.; Cusanovich, M. A.; San Pietro, A. *Biochemistry* **1968,** *7,* 1591.
68. Evans, M. C. W.; Hall, D. O.; Johnson, C. E. *Biochem. J.* **1970,** *119,* 289.
69. Belinski, M.; Bertini, I.; Galas, O.; Luchinat, C. *Z. Naturforsch., A: Phys. Sci.* **1995,** *50,* 75.
70. Bominaar, E. L.; Borshch, S. A.; Girerd, J.-J. *J. Am. Chem. Soc.* **1994,** *116,* 7957.
71. Bominaar, E. L.; Borshch, S. A.; Girerd, J.-J. *J. Am. Chem. Soc.* **1994,** *116,* 5362.
72. Palii, A. V.; Ostrovsky, S. M.; Klokishner, S. I.; Tsukerblat, B. S. *Phys. Lett. A* **1994,** *185,* 480.
73. Bertini, I.; Gaudemer, A.; Luchinat, C.; Piccioli, M. *Biochemistry* **1993,** *32,* 12887.
74. Belinskii, M. *Chem. Phys.* **1993,** *176,* 15.
75. Ueyama, N.; Nakamura, A. *Kikan Kagaku Sosetsu* **1995,** *24,* 44.
76. Tomohiro, T.; Uoto, K.; Kodaka, M.; Shimura, T.; Kubota, Y.; Okada, T.; Okuno, H. *Kagaku Gijutsu Kenkyusho Hokoku* **1992,** *87,* 187.
77. Spiro, T. G.; Hare, J.; Yachandra, V.; Gewirth, A.; Johnson, M. K.; Remsen, E. *Met. Ions Biol.* **1982,** *4,* 407.
78. Noodleman, L.; Peng, C. Y.; Case, D. A.; Mouesca, J.-M. *Coord. Chem. Rev.* **1995,** *144,* 199.
79. Michaels, M. L.; Pham, L.; Nghiem, Y.; Cruz, C.; Miller, J. H. *Nucleic Acids Res.* **1990,** *18,* 3841.
80. Prince, R. C.; Grossman, M. J. *Trends Biochem. Sci.* **1993,** *18,* 153.
81. Cunningham, R. P.; Asahara, H.; Bank, J. F.; Scholes, C. P.; Salerno, J. C.; Surerus, K.; Munk, E.; McCracken, J.; Peisach, J.; Emptage, M. H. *Biochemistry* **1989,** *28,* 4450.
82. Haile, D. J.; Roualt, T. A.; Harford, J. B.; Kennedy, M. C.; Blondin, G. A.; Beinert, H.; Klausner, R. D. *Proc. Natl. Acad. Sci. U.S.A.* **1992,** *89,* 11735.
83. Kennedy, M. C.; Mende-Mueller, L.; Blondin, G. A.; Beinert, H. *Proc. Natl. Acad. Sci. U.S.A.* **1992,** *89,* 11730.
84. Roualt, T. A.; Stout, C. D.; Kaptain, S.; Harford, J. B.; Klausner, R. D. *Cell* **1991,** *64,* 881.
85. Switzer, R. L. *Biofactors* **1989,** *2,* 77.
86. Chang, C. H.; Ballinger, M. D.; Reed, G. H. *Biochemistry* **1996,** *35,* 11081.
87. Emptage, M. H. *in* "Metal Clusters in Proteins"; Que, L., Ed.; ACS: Washington, 1988; Vol. 372, pp. 343–371.

88. Khoroshilova, N.; Beinert, H.; Kiley, P. J. *Proc. Natl. Acad. Sci. U.S.A.* **1995,** *92,* 2499.
89. Beinert, H.; Kiley, P. *FEBS Lett.* **1996,** *382,* 218.
90. Lazazzera, B. A.; Beinert, H.; Khoroshilova, N.; Kennedy, M. C.; Kiley, P. J. *J. Biol. Chem.* **1996,** *271,* 2762.
91. Kerfeld, C. A.; Chan, C.; Hirasawa, M.; Kleis-SanFrancisco, S.; Yeates, T. O.; Knaff, D. B. *Biochemistry* **1996,** *35,* 7812.
92. Hochkoeppler, A.; Kofod, P.; Zannoni, D. *FEBS Lett.* **1995,** *375,* 197.
93. Hochkoeppler, A.; Kofod, P.; Ferro, G.; Ciurli, S. *Arch. Biochem. Biophys.* **1995,** *322,* 313.
94. Schoepp, B.; Parot, P.; Menin, L.; Gaillard, J.; Richaud, P.; Vermeglio, A. *Biochemistry* **1995,** *34,* 11736.
95. Hochkoeppler, A.; Ciurli, S.; Venturoli, G.; Zannoni, D. *FEBS Lett.* **1995,** *357,* 70.
96. Meyer, T. E.; Cannac, V.; Fitch, J.; Bartsch, R. G.; Tollin, D.; Tollin, G.; Cusanovich, M. A. *Biochim. Biophys. Acta* **1990,** *1017,* 125.
97. Butler, J.; Sykes, A.; Buxton, G. V.; Harrington, P. C.; Wilkins, R. G. *Biochem. J.* **1980,** *189,* 641.
98. Burbaev, D. S.; Solozhenkin, I. P.; Zvyagil'skaya, R. A.; Blyumenfel'd, L. A. *Biofizika* **1981,** *26,* 447.
99. Castro, L.; Rodriguez, M.; Radi, R. *J. Biol. Chem.* **1994,** *269,* 29409.
100. Faridoon, K. Y.; Zhuang, H.-Y.; Sykes, A. G. *Inorg. Chem.* **1994,** *33,* 2209.
101. Ramsay, R. R.; Singer, T. P. *Biochemistry* **1984,** *221,* 489.
102. Breiter, D. R.; Meyer, T. E.; Rayment, I.; Holden, H. M. *J. Biol. Chem.* **1991,** *266,* 18660.
103. Ciszewska, H.; Bagyinka, C.; Tigyi, G.; Kovacs, K. L. *Acta Biochim. Biophys. Hung.* **1989,** *24,* 361.
104. Zannoni, D.; Ingledew, W. J. *Arch. Microbiol.* **1983,** *135,* 176.
105. Zorin, N. A.; Gogotov, I. N. *Biokhimiya(Moscow)* **1983,** *48,* 1181.
106. Kennel, S. J.; Bartsch, R. G.; Kamen, M. D. *Biophys. J.* **1972,** *12,* 882.
107. Fukumori, Y.; Yamanaka, T. *Curr. Microbiol.* **1979,** *3,* 117.
108. Bentrop, D.; Bertini, I.; Capozzi, F.; Dikiy, A.; Eltis, L.; Luchinat, C. *Biochemistry* **1996,** *35,* 5928.
109. Carter, C. W.; Kraut, J.; Freer, S. T.; Xuong, N. H.; Alden, R. A.; Bartsch, R. G. *J. Biol. Chem.* **1974,** *249, 4212.*
110. Carter, C. W.; Kraut, J.; Freer, S. T.; Xuong, N. H.; Alden, R. A. *J. Biol. Chem.* **1974,** *249,* 6339.
111. Breiter, D. R. *Diss. Abstr. Int. B 1992* ***1991,*** *53,* 1383.
112. Banci, L.; Bertini, I.; Eltis, L. D.; Felli, I.; Kastrau, D. H. W.; Luchinat, C.; Piccioli, M.; Pierattelli, R.; Smith, M. *Eur. J. Biochem.* **1994,** *225,* 715.
113. Benning, M. M.; Meyer, T. E.; Rayment, I.; Holden, H. M. *Biochemistry* **1994,** *33,* 2476.
114. Rayment, I.; Wesenberg, G.; Meyer, T. E.; Cusanovich, M. A.; Holden, H. M. *J. Mol. Biol.* **1992,** *228,* 672.
115. Moulis, J.-M.; Davasse, V.; Golinelli, M.-P.; Quinkal, I. *J. Biol. Inorg. Chem.* **1996,** *1,* 2.
116. Banci, L.; Bertini, I.; Dikiy, A.; Kastrau, D. H.; Luchinat, C.; Sompornpisut, P. *Biochemistry* **1995,** *34,* 206.
117. Cowan, J. A. "Inorganic Biochemistry: An Introduction"; Cowan, J. A., Ed.; VCH: New York, 1993; Chap. 5.

*118.* Berg, J. M.; Holm, R. H. *in* "Metal Ions in Biology"; Spiro, T. G., Ed.; Wiley Interscience: New York, 1982; Vol. 4, pp. 1–66.
*119.* Stout, C. D., *in* "Metal Ions in Biology"; Spiro, T. G., Ed.; John Wiley and Sons: New York, 1982; Vol. 4, pp. 97–146.
*120.* Cammack, R. *Adv. Inorg. Chem.* **1992,** *38,* 281.
*121.* Beinert, H. *FASEB J.* **1990,** 42483.
*122.* Matsubara, H.; Saeki, K. *Adv. Inorg. Chem.* **1992,** *38,* 223.
*123.* Moulis, J. M.; Scherrer, N.; Gagnon, J.; Forest, E.; Petillot, Y.; Garcia, D. *Arch. Biochem. Biophys.* **1993,** *305,* 186.
*124.* Adman, E.; Watenpaugh, K. D.; Jensen, L. H. *Proc. Natl. Acad. Sci. U.S.A.* **1975,** *72,* 4854.
*125.* Sweeney, W. V.; Magliozzo, R. S. *Biopolymers* **1980,** *19,* 2133.
*126.* Mizrahi, I. A.; Meyer, T. E.; Cusanovich, M. A. *Biochemistry* **1980,** *19,* 4727.
*127.* Bertini, I.; Gaudemer, A.; Luchinat, C.; Piccioli, M. *Biochemistry* **1993,** *32,* 12887.
*128.* Agarwal, A.; Tan, J.; Eren, M.; Tevelev, A.; Lui, S. M.; Cowan, J. A. *Biochem. Biophys. Res. Commun.* **1993,** *197,* 1357.
*129.* Eltis, L. D.; Iwagami, S. G.; Smith, M. *Protein Eng.* **1994,** *7,* 1145.
*130.* Bian, S.; Hille, C. R.; Hemman, C.; Cowan, J. A. *Biochemistry* **1996,** *35,* 14544.
*131.* Agarwal, A.; Li, D.; Cowan, J. A. *Proc. Natl. Acad. Sci. U.S.A.* **1995,** *92,* 9440.
*132.* Shen, B.; Jollie, D. R.; Diller, T. C.; Stout, C. D.; Stephens, P. J.; Burgess, B. K. *Proc. Natl. Acad. Sci. U.S.A.* **1995,** *92,* 10064.
*133.* Kowal, A. T.; Werth, M. T.; Manodori, A.; Cecchini, G.; Schroeder, I.; Gunsalus, R. P.; Johnson, M. K. *Biochemistry* **1995,** *34,* 12284.
*134.* Iwagami, S. G.; Creagh, A. L.; Haynes, C. A.; Borsari, M.; Felli, I. C.; Piccioli, M.; Eltis, L. D. *Can. Protein Sci.* **1995,** *4,* 2562.
*135.* Li, D.; Cottrell, C. E.; Cowan, J. A. *J. Protein Chem.* **1995,** *14,* 115.
*136.* Lui, S. M.; Cowan, J. A. *J. Am. Chem. Soc.* **1994,** *116,* 4483.
*137.* Bertini, I.; Felli, I.; Kastrau, D. H. W.; Luchinat, C.; Piccioli, M.; Viezzoli, M. S. *Eur. J. Biochem.* **1994,** *225,* 703.
*138.* Bartsch, R. G. *Methods Enzymol.* **1978,** *53,* 329.
*139.* Maskiewicz, R.; Bruice, T. C. *Proc. Natl. Acad. Sci. U.S.A.* **1977,** *74,* 5321.
*140.* Nakamoto, M.; Tanaka, K.; Tanaka, T. *J. Chem. Soc., Chem. Commun.* **1988,** *21,* 1422.
*141.* O'Sullivan, T.; Millar, M. M. *J. Am. Chem. Soc.* **1985,** *107,* 4096.
*142.* Roth, E. K. H.; Jordanov, J. *Inorg. Chem.* **1992,** *31,* 240.
*143.* Blonk, H. L.; Kievit, O.; Roth, E. K.-H.; Jordanov, J.; van der Linden, J. G. M.; Steggerda, J. J. *Inorg. Chem.* **1991,** *30,* 3231.
*144.* Kambayashi, H.; Nagao, H.; Tanaka, K.; Nakamoto, M.; Peng, S.-M. *Inorg. Chim. Acta* **1993,** *209,* 143.
*145.* Chothia, C. *Nature* **1975,** *254,* 304.
*146.* Soriano, A.; Cowan, J. A. *Inorg. Chim. Acta* **1996,** *251,* 285.
*147.* Babini, E.; Bertini, I.; Borsari, M.; Capozzi, F.; Dikiy, A.; Eltis, L. D.; Luchinat, C. *J. Am. Chem. Soc.* **1996,** *118,* 75.
*148.* Agarwal, A.; Li, D.; Cowan, J. A. *J. Am. Chem. Soc.* **1996,** *118,* 927.
*149.* Li, D.; Agarwal, A.; Cowan, J. A. *Inorg. Chem.* **1996,** *35,* 1121.
*150.* Bertini, I.; Luchinat, C. "NMR of Paramagnetic Substances"; Bertini, I., and Luchinat, C., Eds.; Elsevier: New York, 1996; Vol. 150, pp. 185–220.
*151.* Gerig, J. T. *Methods Enzymol.* **1986,** *177,* 3.
*152.* Gerig, J. T. *Prog. Nucl. Magn. Reson.* **1994,** *26,* 293.
*153.* Gerig, J. T. *Bio. Magn. Reson.* **1978,** *1,* 139.

*154.* Hansen, P. E.; Dettman, H. D.; Sykes, B. D. *J. Magn. Reson.* **1985,** *62,* 487.
*155.* Soriano, A.; Li, D.; Bian, S.; Agarwal, A.; Cowan, J. A. *Biochemistry* **1996,** *35,* 12479.
*156.* Bertrand, P.; Mbarki, O.; Blanchard, L.; Guerlesquin, F.; Tegoni, M. *Biochemistry* **1995,** *34,* 11071.
*157.* Bertini, I.; Briganti, F.; Luchinat, C.; Scozzafava, A.; Sola, M. *J. Am. Chem. Soc.* **1991,** *113,* 1237.
*158.* Cammack, R. *Biochem. Biophys. Res. Commun.* **1973,** *54,* 548.
*159.* Ambler, R. P.; Meyer, T. E.; Kamen, M. D. *Arch. Biochem. Biophys.* **1993,** *306,* 215.
*160.* Banci, L.; Bertini, I.; Ciurli, S.; Luchinat, C.; Pierattelli, R. *Inorg. Chim. Acta* **1995,** *240,* 251.
*161.* Luchinat, C.; Capozzi, F.; Borsari, M.; Battistuzzi, G.; Sola, M. *Biochem. Biophys. Res. Commun.* **1994,** *203,* 436.
*162.* Heering, H. A.; Bulsink, Y. B. M.; Hagen, W. R.; Meyer, T. E. *Biochemistry* **1995,** *34,* 14675.
*163.* Carter, C. W. J. *J. Biol. Chem.* **1977,** *252,* 7802.
*164.* Kassner, R. J.; Yang, W. *J. Am. Chem. Soc.* **1977,** *99,* 4351.
*165.* Taniguchi, V. T.; Malmstrom, B. G.; Anson, F. C.; Gray, H. B. *Proc. Natl. Acad. Sci. U.S.A.* **1982,** *79,* 3387.
*166.* Taniguchi, V. T.; Ellis, W. R. J.; Cammarata, V.; Webb, J.; Anson, F. C.; Gray, H. B.; "Electrochemical and Spectrochemical Studies of Biological Redox Components"; Amer. Chem. Soc.: Washington, D.C., 1982; p. 51.
*167.* Mizrahi, I. A.; Cusanovich, M. A. *Biochemistry* **1980,** *19,* 4733.
*168.* Beratan, D. N.; Betts, J. N.; Onuchic, J. N. *Science* **1991,** *252,* 1285.
*169.* Jensen, G. M.; Warshel, A.; Stephens, P. J. *Biochemistry* **1994,** *33,* 10911.
*170.* Churg, A. K.; Warshel, A. *Biochemistry* **1986,** *25,* 1675.
*171.* Warshel, A.; Russell, S. T. *Q. Rev. Biophys.* **1984,** *17,* 283.
*172.* Meyer, T. E. *Methods Enzymol.* **1994,** *243,* 435.
*173.* Tedro, S. M.; Meyer, T. E.; Bartsch, R. G.; Kamen, M. D. *J. Biol. Chem.* **1981,** *256,* 731.
*174.* Ciszewska, H.; Bagyinka, C.; Kovacs, K. L. *Biokonvers. Soln. Energ., Mater. Mezhdunar. Simp.* **1984,** 330.
*175.* Wermter, U.; Fischer, U. *Bioscience* **1983,** 38C, 986.
*176.* Tedro, S. M.; Meyer, T. E.; Kamen, M D. *J. Biol. Chem.* **1974,** *249,* 1182.
*177.* Tedro, S. M.; Meyer, T. E.; Kamen, M. D. *Arch. Biochem. Biophys.* **1985,** *241,* 656.
*178.* Tedro, S. M.; Meyer, T. E.; Kamen, M. D. *J. Biol. Chem.* **1977,** *252,* 7826.
*179.* Kusano, T.; Takeshima, T.; Sugawara, K.; Inoue, C.; Shiratori, T.; Yano, T.; Fukumori, Y.; Yamanaka, T. *J. Biol. Chem.* **1992,** *267,* 11242.
*180.* Kusano, T.; Takeshima, T.; Sugawara, K.; Inoue, C.; Shiratori, T.; Yano, T.; Fukumori, Y.; Yamanaka, T. *Biohydrometall. Technol., Proc. Int. Biohydrometall. Symp.* **1993,** *2,* 725.
*181.* Stombaugh, N. A.; Sundquist, J. E.; Burris, R. H.; Orme-Johnson, W. H. *Biochemistry* **1976,** *15,* 2633.
*182.* Fukuyama, K.; Matsubara, H.; Tsukihara, T.; Katsube, Y. *J. Mol. Biol.* **1989,** *210,* 383.